

European Association of Echocardiography recommendations for the assessment of valvular regurgitation. Part 2: mitral and tricuspid regurgitation (native valve disease)

Patrizio Lancellotti (Chair)^{1*}, Luis Moura², Luc A. Pierard¹, Eustachio Agricola³, Bogdan A. Popescu⁴, Christophe Tribouilloy⁵, Andreas Hagendorff⁶, Jean-Luc Monin⁷, Luigi Badano⁸, and Jose L. Zamorano⁹ on behalf of the European Association of Echocardiography

Document Reviewers: Rosa Sicari^a, Alec Vahanian^b, and Jos R.T.C. Roelandt^c

¹Department of Cardiology, Valvular Disease Clinic, University Hospital, Université de Liège, CHU du Sart Tilman, 4000 Liège, Belgium; ²Oporto Medical School, Porto, Portugal; ³Division of Noninvasive Cardiology, San Raffaele Hospital, IRCCS, Milan, Italy; ⁴Department of Cardiology, 'Carol Davila' University of Medicine and Pharmacy, Bucharest, Romania; ⁵Department of Cardiology, University Hospital of Amiens, Picardie, France; ⁶Department für Innere Medizin, Kardiologie, Leipzig, Germany; ⁷Cardiologie/Maladie Valvulaires Cardiaques Laboratoire d'échocardiographie CHU Henri Mondor, Créteil, France; ⁸Department of Cardiology, University of Padova, Padova, Italy; ⁹University Clinic San Carlos, Madrid, Spain

^aInstitute of Clinical Physiology, PISA, Italy; ^bHôpital Bichat, Paris, France; and ^cDepartment of Cardiology, Thoraxcentre, Erasmus MC, Rotterdam, The Netherlands

Received 11 February 2010; accepted after revision 15 February 2010

Mitral and tricuspid are increasingly prevalent. Doppler echocardiography not only detects the presence of regurgitation but also permits to understand mechanisms of regurgitation, quantification of its severity and repercussions. The present document aims to provide standards for the assessment of mitral and tricuspid regurgitation.

Keywords Valvular regurgitation • Echocardiography • Recommendations • Mitral valve • Tricuspid valve

Introduction

The second part of the recommendations on the assessment of valvular regurgitation focuses on mitral regurgitation (MR) and tricuspid regurgitation (TR). As for the first part, the present document is based upon a consensus of experts.¹ It provides clues not only for MR and TR quantification but also elements on the assessment of valve anatomy and cardiac function.

Mitral regurgitation

MR is increasingly prevalent in Europe despite the reduced incidence of rheumatic disease.² The development of surgical mitral valve repair introduced in the early seventies by Alain Carpentier has dramatically changed the prognosis and the management of

patients presenting with severe MR. The possibility of repairing the mitral valve imposes new responsibilities on the assessment of MR by imaging which should provide precise information on type and extent of anatomical lesions, mechanisms of regurgitation, aetiology, amount of regurgitation, and reparability of the valve. It is essential to distinguish between organic (primary) and functional (secondary) MR which radically differs in their pathophysiology, prognosis, and management.

Anatomy and function of the mitral valve

Normal mitral valve function depends on perfect function of the complex interaction between the mitral leaflets, the subvalvular apparatus (chordae tendineae and papillary muscles), the mitral annulus, and the left ventricle (LV). An imperfection in any one of these components can cause the valve to leak.³

* Corresponding author. Tel: +32 4 366 71 94, Fax: +32 4 366 71 95, Email: plancellotti@chu.ulg.ac.be

Published on behalf of the European Society of Cardiology. All rights reserved. © The Author 2010. For permissions please email: journals.permissions@oxfordjournals.org.

Valvular leaflets

The normal mitral valve has two leaflets (each with a thickness about 1 mm) that are attached at their bases to the fibromuscular ring, and by their free edges to the subvalvular apparatus. The posterior leaflet has a quadrangular shape and is attached to approximately two-thirds of the annular circumference; the anterior leaflet attaches to the remaining one-third (Figure 1). The posterior leaflet typically has two well defined indentations which divide the leaflet into three individual scallops identified as P1, P2, and P3. The P1 scallop corresponds to the external, anterolateral portion of the posterior leaflet, close to the anterior commissure and the left atrium (LA) appendage. The P2 scallop is medium and more developed. The P3 scallop is internal, close to the posterior commissure and the tricuspid annulus. The anterior leaflet has a semi-circular shape and is in continuity with the non-coronary cusp of the aortic valve, referred to as the intervalvular fibrosa. The free edge of the anterior leaflet is usually continuous, without indentations. It is artificially divided into three portions A1, A2, and A3, corresponding to the posterior scallops P1, P2, and P3. The commissures define a distinct area where the anterior and posterior leaflets come together at their insertion into the annulus. Sometimes the commissures exist as well defined leaflet segments, but more often this area is a subtle region. When the mitral valve is closed, the line of contact between the leaflets is termed coaptation line and the region of leaflet overlap is called the zone of apposition.

By echocardiography, the presence and the extent of inadequate tissue (e.g. calcifications), of excess leaflet tissue and the precise localization of the leaflet lesions should be analysed. Describing the mitral valve segmentation is particularly useful to precisely define the anatomical lesions and the prolapsing segments in patients with degenerative MR. For this purpose, transoesophageal echocardiography (TEE) still remains the recommended approach in many laboratories. However, in experienced hands, functional assessment of MR by transthoracic echocardiography (TTE) predicts accurately valve reparability. Images with both approaches are recorded using appropriate standardized views (Figures 2–6).⁴

The short-axis view can be obtained by TTE or TEE, using the classical parasternal short-axis view and the transgastric view at 0°. This view permits in diastole the assessment of the six scallops and the two commissures. In systole, the localization of prolapse may be identified by the localization of the origin of the regurgitant jet.

With TTE, a classical apical four-chamber view is obtained and explores the anterior leaflet, the segments A3 and A2 and the posterior leaflet in its external scallop P1. With TEE, different valvular segments are observed which depend on the position of the probe in the oesophagus which progresses from up to down. This permits to observe successively A1 and P1 close to the anterolateral commissure, A2 and P2 and finally A3 and P3 close to the posteromedial commissure (at 40–60°).

Parasternal long-axis view with TTE and sagittal view at 120° with TEE show the medium portions of the leaflets (A2 and P2). A bi-commissural view can be obtained in the apical two-chamber view with TTE and a view at 40–60° with TEE showing the two commissural regions and from left to right P3, A2, and P1. A two-chamber view from the transgastric position, perpendicular to the subvalvular apparatus permits to measure the length of the

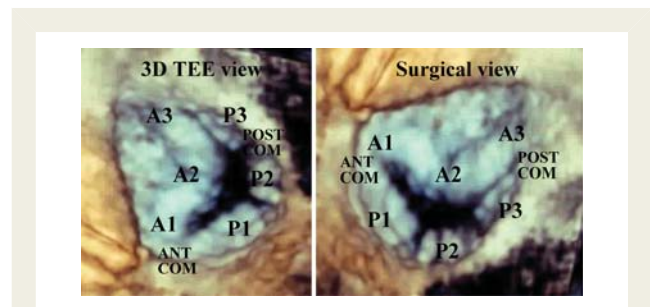


Figure 1 Real-time 3D transoesophageal echocardiography volume rendering of the mitral valve. Left: classical transoesophageal echocardiography view; right: surgical view. A1, A2, A3, anterior mitral valve scallops; P1, P2, P3, posterior mitral valve scallops; ANT COMM, anterolateral commissure; POST COMM, posteromedial commissure.

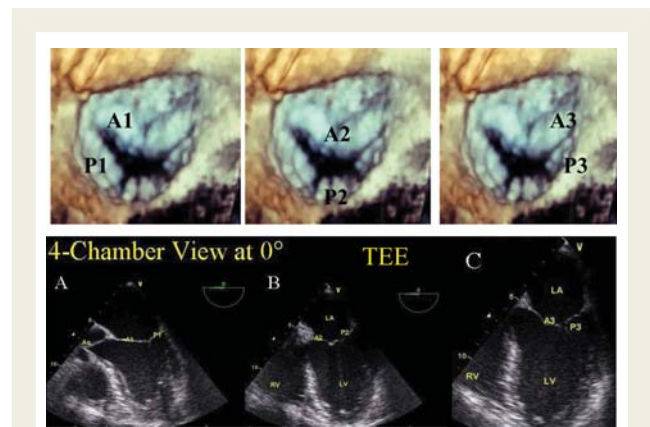


Figure 2 Mitral valvular segmentation analysis with 2D transoesophageal echocardiography. Views obtained at 0°: (A) Five-chamber view depicting A1 and P1, (B) four-chamber view depicting A2 and P2; (C) downward four-chamber view depicting A3 and P3.

chordae and the distances between the head of the papillary muscle and the mitral annulus.

Real-time 3D TTE and/or TEE provide comprehensive visualization of the different components of the mitral valve apparatus and is probably the method of choice when available.⁵ Real-time 3D TEE is particularly useful in the dialogue between the echocardiographer and the surgeon. Multiple views are available which permit to precisely determine the localization and the extent of prolapse. The 'en face' view seen from the LA perspective is identical to the surgical view in the operating room. This view allows to perfectly analysing the extent of commissural fusion in rheumatic MR. The leaflet involvement in degenerative myxomatous disease is visualized by 3D echo as bulging or protrusion of one or more segments of a single or multiple mitral valve leaflets. In addition, the presence of chordal rupture and extension of the concomitant annular dilation can be assessed in the same view. Preoperatively, the measurement by 3D echo of the surface of the anterior leaflet could help to define the size of the annular ring.

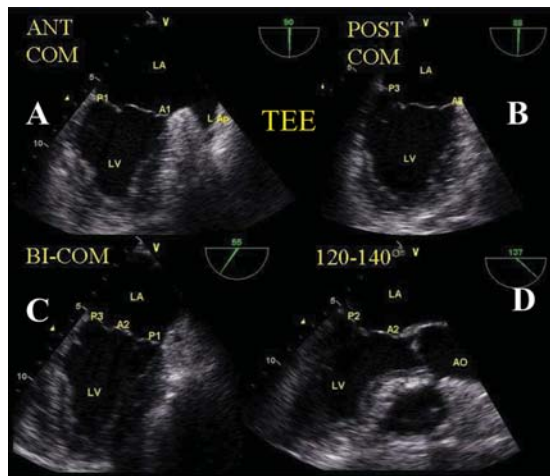


Figure 3 Mitral valvular segmentation analysis with 2D transoesophageal echocardiography. (A) Two-chamber view with a counter clock wise mechanical rotation permitting to visualize A1, P1, and the anterolateral commissure. (B) Two-chamber view with a clock wise mechanical rotation permitting to visualize A3, P3, and the posteromedial commissure. (C) Bicommisural view. (D) View at 120° visualizing A2 and P2.

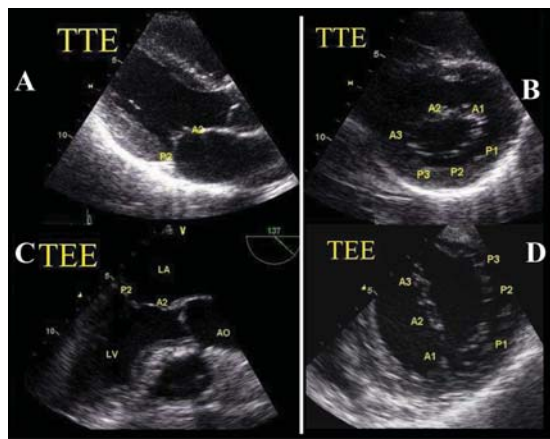


Figure 4 Mitral valvular segmentation analysis with 2D transoesophageal echocardiography (TEE) and transthoracic echocardiography (TTE). (A) 2D TTE parasternal long-axis view depicting A2 and P2. (B) 2D TTE parasternal short-axis view depicting each scallop. (C) 2D TEE view at 120° visualizing A2 and P2. (D) 2D TEE the transgastric view at 0° depicting each scallop.

Mitral annulus

The mitral annulus constitutes the anatomical junction between the LV and the LA, and serves as insertion site for the leaflet tissue. It is oval and saddle shaped.⁶ The anterior portion of the mitral annulus is attached to the fibrous trigones and is generally more developed than the posterior annulus. Both parts of the annulus may dilate in pathologic conditions. The anterior–posterior diameter can be measured using real-time 3D or by conventional 2D in the

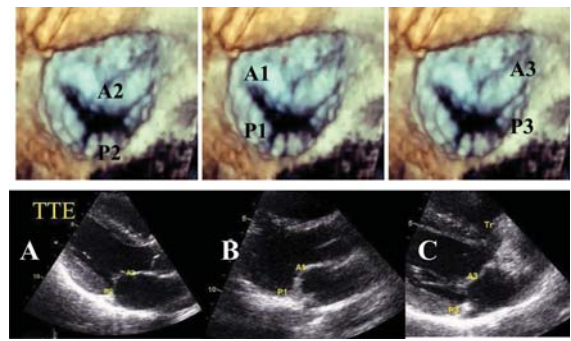


Figure 5 2D transthoracic echocardiography of parasternal long-axis view. (A) A2 and P2. (B) A1 and P1 (tilting of the probe toward the aortic valve). (C) A3 and P3 (tilting of the probe toward the tricuspid (Tr) valve).

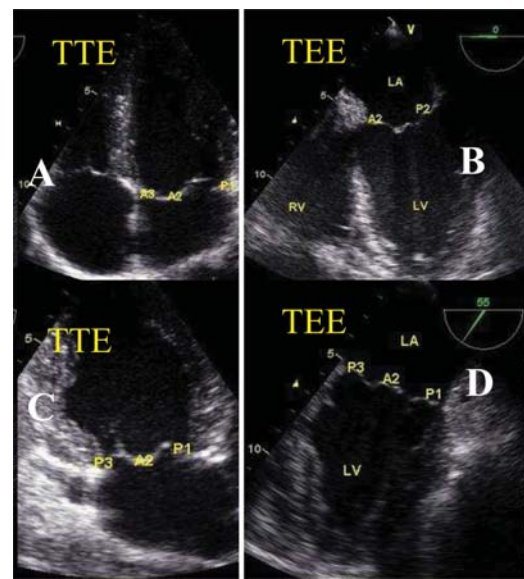


Figure 6 Mitral valvular segmentation analysis with 2D transoesophageal echocardiography (B and D) and transthoracic echocardiography (A and C). (A) Four-chamber view depicting A3, A2, and P1 and (C) bicommisural view. For B and D see above.

parasternal long-axis view. The diameter is compared with the length of the anterior leaflet measured in diastole. Annular dilatation is present when the ratio annulus/anterior leaflet is >1.3 or when the diameter is >35 mm.⁷ The presence and extent of annular calcification is an important parameter to describe. The normal motion and contraction of the mitral annulus also contributes to maintaining valve competence. The normal contraction of the mitral annulus (decrease in annular area in systole) is 25%.⁸

Chordae tendineae

There are three sets of chordae arising from the papillary muscles. They are classified according to their site of insertion between the free margin and the base of leaflets. Marginal chordae (primary

chordae) are inserted on the free margin of the leaflets and function to prevent prolapse of the leaflet margin. Intermediate chordae (secondary chordae) insert on the ventricular surface of the leaflets and relieve valvular tissue of excess tension. Often two large secondary or 'strut' chordae can be individualized. They may be important in preserving ventricular shape and function. Basal chordae (tertiary chordae) are limited to the posterior leaflet and connect the leaflet base and mitral annulus to the papillary muscle. Additional commissural chordae arise from each papillary muscle. Rupture, calcification, fusion, or redundancy of the chordae can lead to regurgitation.

Papillary muscles

Because the annulus resides in the left atrioventricular furrow, and the chordae tendineae are connected to the LV via the papillary muscles, mitral valve function is intimately related to LV function. There are two papillary muscles arising from the LV: the anterolateral papillary muscle is often composed of one body or head, and the posteromedial papillary muscle usually with two bodies or heads. Rupture, fibrotic elongation or displacement of the papillary muscles may lead to MR.

Mitral valve analysis: recommendations

- (1) TTE is recommended as the first-line imaging modality for mitral valve analysis.
- (2) TEE is advocated when TTE is of non-diagnostic value or when further diagnostic refinement is required.
- (3) 3D-TEE or TTE is reasonable to provide additional information in patients with complex mitral valve lesion.
- (4) TEE is not indicated in patients with a good-quality TTE except in the operating room when a mitral valve surgery is performed.

Key point

Valve analysis should integrate the assessment of the aetiology, the lesion process and the type of dysfunction. The distinction between a primary and a secondary cause of MR is mandatory. The diameter of the mitral annulus, the leaflet involved in the disease process and the associated valvular lesions should be carefully described in the final report.

Aetiology and mechanism of mitral regurgitation

Causes and mechanisms of MR are not synonymous. A particular cause might produce regurgitation by different mechanisms. MR is roughly classified as organic (primary) or functional (secondary). Organic MR is due to intrinsic valvular disease whereas functional MR is caused by regional and/or global LV remodelling without structural abnormalities of the mitral valve. Causes of primary MR include most commonly degenerative disease (Barlow, fibroelastic degeneration, Marfan, Ehler's-Danlos, annular calcification), rheumatic disease, and endocarditis. Ruptured papillary muscle

secondary to myocardial infarction defined an organic ischaemic MR. Causes of secondary MR include ischaemic heart disease and cardiomyopathy.

Aetiology

Degenerative mitral regurgitation

Degenerative disease is the most common aetiology of MR. Several terms are used that should be distinguished: (i) A *billowing* valve is observed when a part of the mitral valve body protrudes into the LA; the coaptation is, however, preserved beyond the annular plane. MR is usually mild in this condition; (ii) A *floppy* valve is a morphologic abnormality with thickened leaflet (diastolic thickness >5 mm) due to redundant tissue; (iii) Mitral valve *prolapse* implies that the coaptation line is behind the annular plane. With 2D echo, the diagnosis of prolapse should be made in the parasternal or eventually the apical long-axis view, but not in the apical four-chamber view, because the saddle shaped annulus may lead to false positive diagnosis (Figure 7). The most common phenotype of mitral prolapse is diffuse myxomatous degeneration (Barlow's disease; Figures 8 and 9); (iv) *Flail leaflet*: this term is used when the free edge of a leaflet is completely reversed in the LA (the leaflet tip is directed towards the LA while in prolapse it is directed towards the LV). Flail leaflet is usually a consequence of ruptured chordae (degenerative MR or infective endocarditis). It affects more frequently the posterior leaflet (>70% of cases) and is usually associated with severe MR.

Rheumatic mitral regurgitation

Rheumatic MR is characterized by variable thickening of the leaflets especially at the level of their free edge. Fibrosis of the chordae is frequent, especially of those attached to the posterior valve explaining the rigidity and reduced motion of the posterior leaflet in diastole. In some patients, the posterior leaflet remains

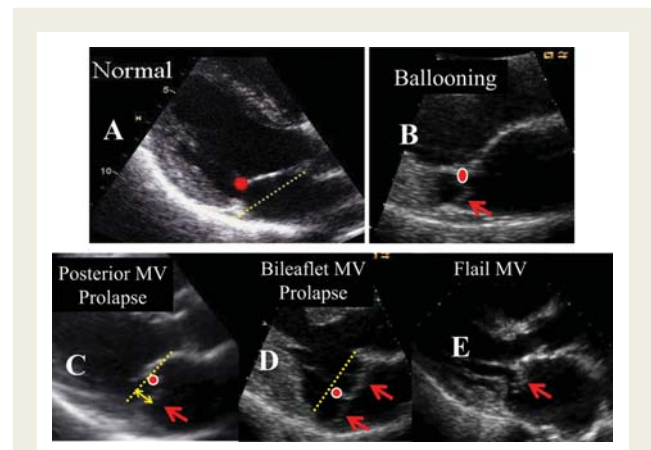


Figure 7 (A) In normal mitral valve, the coaptation (red point) occurs beyond the mitral annular plane (line); (B) billowing mitral valve is observed when a part of the mitral valve body protrudes into the left atrium (arrow); (C and D) mitral valve prolapse is defined as abnormal systolic displacement of one (C: posterior prolapse) or both leaflets into the left atrium below the annular (D: bileaflet prolapse); (E) flail of the anterior leaflet (arrow).

in a semi-open position throughout the cardiac cycle and the motion of the anterior leaflet in systole produces a false aspect of prolapse.

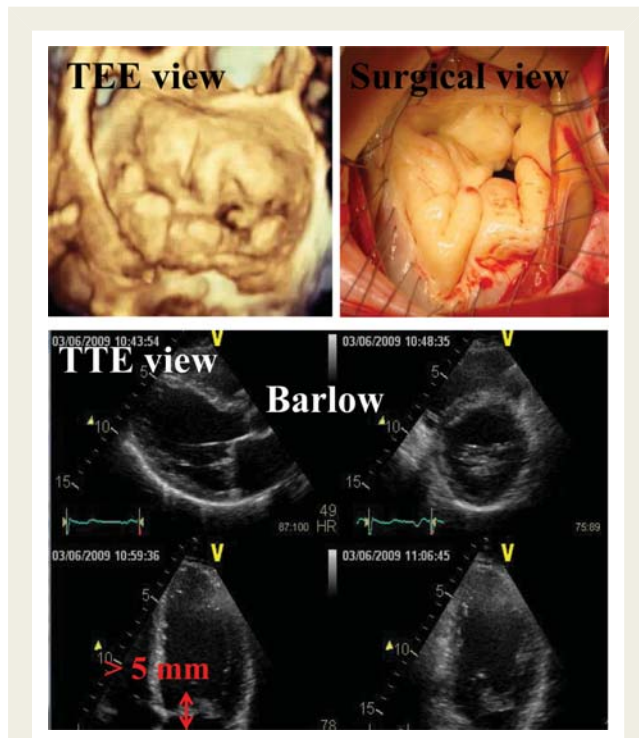


Figure 8 Example of severe Barlow's disease with redundant and thickened mitral valve.

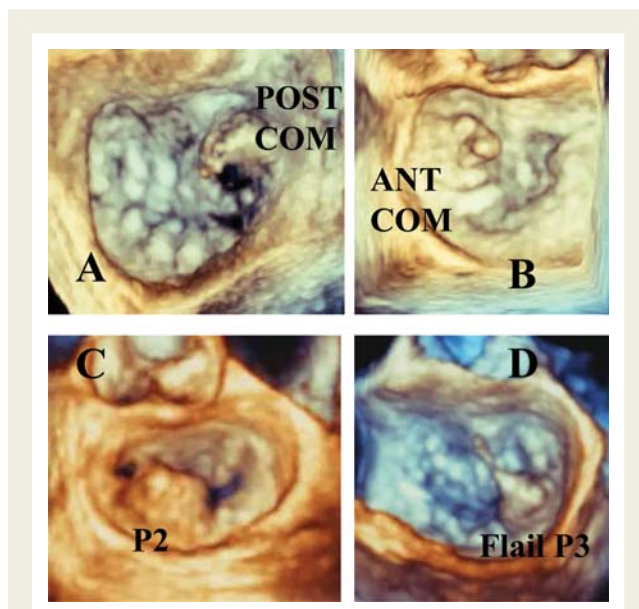


Figure 9 3D-transoesophageal echocardiography rendering of the mitral valve. (A) Posteromedial (POST-COMM) commissure prolapse; (B) anterolateral (ANT-COMM) commissure prolapse; (C) P2 prolapse; (D) flail of P3.

Functional mitral regurgitation

Functional MR broadly denotes abnormal function of normal leaflets in the context of impaired ventricular function resulting from ischaemic heart disease or dilated cardiomyopathy.⁹ It results from an imbalance between tethering forces—annular dilatation, LV dilatation, papillary muscles displacement, LV sphericity—and closing forces—reduction of LV contractility, global LV dyssynchrony, papillary muscle dyssynchrony, altered mitral systolic annular contraction. Chronic functional ischaemic MR results, in 95% of the cases, from a type IIIb (systolic restriction of leaflet motion) dysfunction. The restrictive motion occurs essentially during systole and is most frequent in patients with previous posterior infarction (asymmetric pattern; *Figure 10*).¹⁰ In this setting, the traction on the anterior leaflet by secondary chordae can induce the so called 'seagull sign'. In patients with idiopathic cardiomyopathy or with both anterior and inferior infarctions, both leaflets exhibit a reduced systolic motion leading to incomplete coaptation (symmetric pattern; *Figure 11*). Rarely, in ischaemic

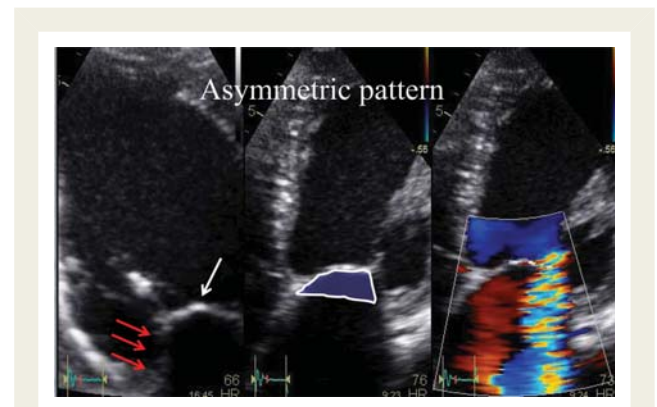


Figure 10 Ischaemic mitral regurgitation with a predominant posterior leaflet restriction (arrows) leading to an asymmetric tenting pattern. The restriction on the anterior leaflet due excessive stretching by the strut chordate provides the typical seagull sign (white arrow). The colour jet is originating centrally but is directed laterally toward the lateral wall of the left atrium.

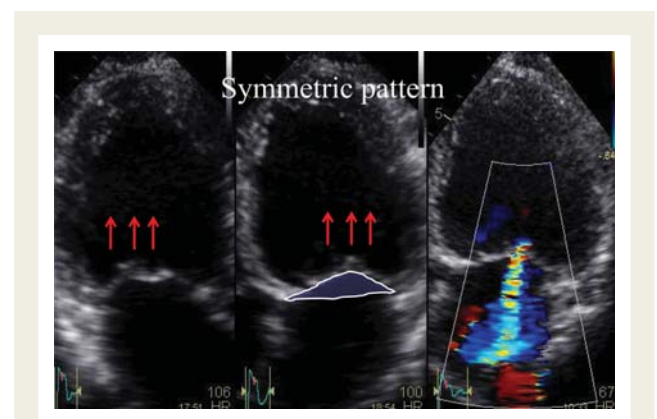


Figure 11 Ischaemic mitral regurgitation with a bileaflet restriction (arrows) leading to a symmetric tenting pattern. The colour jet is originating and directed centrally into the left atrium.

MR, the mechanism of MR is related to fibrosis and elongation of the papillary muscle (Figure 12). On echo, the LV is dilated and more spherical. The annulus is also usually dilated, becomes more circular with lack of dynamic systolic contraction. A number of anatomic measurements can be made that reflect the pathophysiology of functional MR, including global and regional

LV remodelling and the severity of altered geometry of the mitral valve apparatus (tenting area and coaptation distance; Figure 13).¹¹ The location and extent of regional and global LV dysfunction are easily assessed in the classical views (parasternal long-axis and short-axis and apical two, three, and four chamber views). Thin (diastolic thickness <5.5 mm) and hyper-echogenic ventricular segments usually imply the presence of transmural infarction. Global LV remodelling is quantified by the measurements of LV volumes and the calculation of the LV sphericity index. Regional remodelling is quantified by the posterior and lateral displacements of one or both papillary muscles. The tenting area is measured in mid-systole as the area between the mitral annulus and the mitral leaflets body. The tenting area is measured in mid-systole as the area between the mitral annulus and the mitral leaflets body. The apical displacement of the coaptation point (coaptation distance) represents the distance between the mitral annular plane and the point of coaptation.

Mechanisms of mitral regurgitation

Precise determination of the mechanism of MR is an essential component of the echocardiographic examination, in particular when mitral valve repair is considered. The Capentier’s functional classification is often used: (i) Type I: MR is determined by leaflet perforation (infective endocarditis) or more frequently by annular dilatation; (ii) Type II: Excessive leaflet mobility accompanied by displacement of the free edge of one or both leaflets beyond the

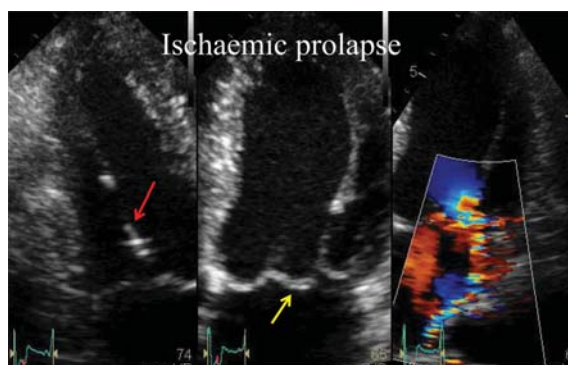


Figure 12 Ischaemic mitral regurgitation due to ischaemic elongation of the posteromedial papillary muscle (red arrow). Yellow arrow: anterior leaflet prolapse.

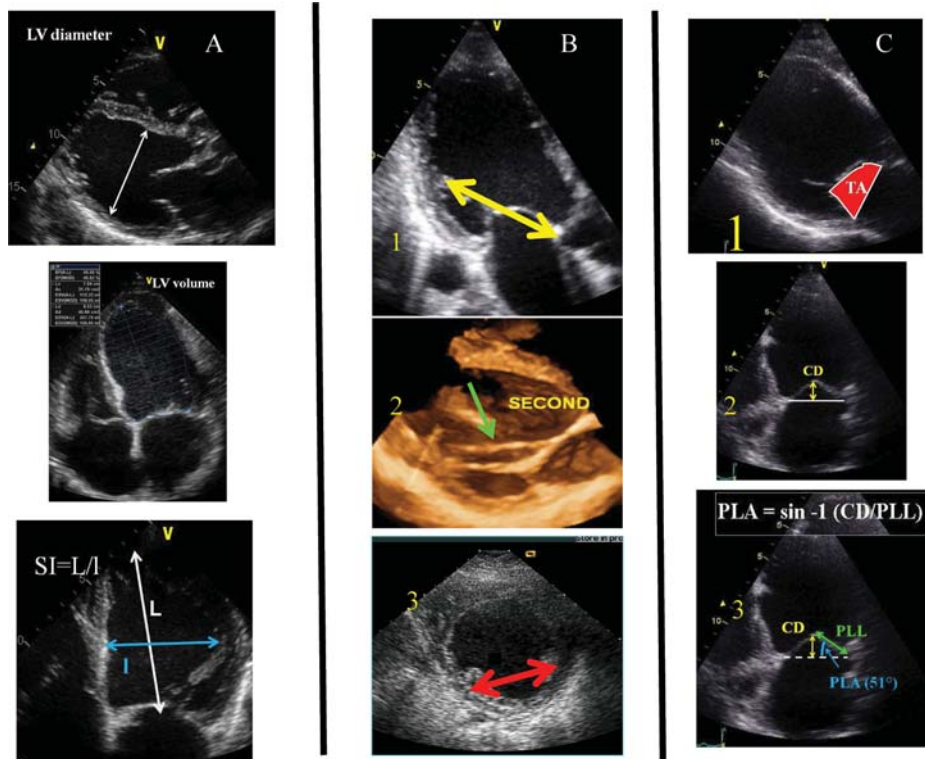


Figure 13 Echo morphologic parameters that are measured in ischaemic mitral regurgitation. (A) Global left ventricle remodelling [diameter, left ventricle (LV) volumes, sphericity index ($SI = L/1$; L, major axis; 1, minor axis)]. (B) Local LV remodelling (1, apical displacement of the posteromedial papillary muscle; 2, second order chordate; 3, interpapillary muscle distance). (C) Mitral valve deformation (1, systolic tenting area (TA); 2, coaptation distance (CD); 3, posterolateral angle (PLA)).

mitral annular plane (mitral valve prolapse); (iii) Type III: The type III is subdivided into type IIIa implying restricted leaflet motion during both diastole and systole due to shortening of the chordae and/or leaflet thickening such as in rheumatic disease, and type IIIb when leaflet motion is restricted only during systole (Figure 14).

Predictors of successful valve repair

Several echocardiographic parameters can help to identify patients at risk of treatment failure. In organic MR, some predictors of unsuccessful repair have been reported: the presence of a large central regurgitant jet, severe annular dilatation (>50 mm), involvement of ≥ 3 scallops especially if the anterior leaflet is involved, and extensive valve calcification (Table 1).¹² Moreover, lack of valve tissue is also an important predictor of unsuccessful repair both in

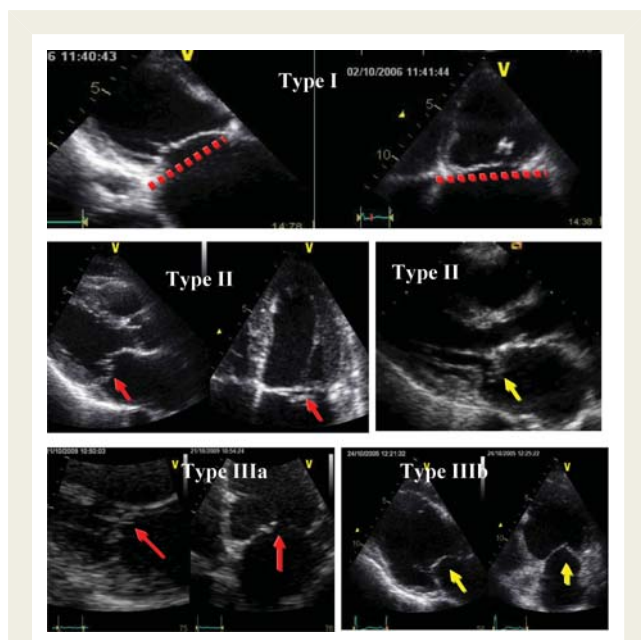


Figure 14 Mechanisms of mitral regurgitation according to the Capentier's functional classification.

rheumatic valve disease and in patients who have had infective endocarditis with large valve perforation.

In functional ischaemic MR, per-operatively (TEE), patients with a mitral diastolic annulus diameter ≥ 37 mm, a systolic tenting area ≥ 1.6 cm² and a severe functional ischaemic MR could have a 50% probability of failure during follow-up.¹³ Pre-operatively (TTE), a coaptation distance >1 cm, a systolic tenting area >2.5 cm², a posterior leaflet angle >45° (indicating a high posterior leaflet restriction), a central regurgitant jet (indicating a severe restriction of both leaflets in patients with severe functional ischaemic MR), the presence of complex jets originating centrally and posteromedially, and a severe LV enlargement (low likelihood of reverse LV remodelling after repair and poor late outcome) increase the risk of mitral valve repair failure. Taking these parameters altogether could reduce the frequency of postoperative functional ischaemic MR recurrence (Table 2).¹¹

Key point

The echocardiographic report should provide clues on the likelihood of valve repair.

Risk of systolic anterior motion after mitral valve surgery

The development of systolic anterior motion (SAM) of the mitral valve with LV outflow tract obstruction after mitral valve repair can lead to severe post-operative haemodynamic instability. Factors predisposing patients to SAM are the presence of a myxomatous mitral valve with redundant leaflets (excessive anterior leaflet tissue), a non-dilated hyperdynamic LV, and a short distance between the mitral valve coaptation point and the ventricular septum after repair.

Assessment of mitral regurgitation severity

Colour flow Doppler

Colour flow imaging

Colour flow imaging, although less accurate, is the most common way to assess MR severity.¹⁴ The general assumption is that as the severity of the MR increases, the size and the extent of the jet into the LA also increases. Theoretically, larger colour jets that extend deep into the LA represent more MR than small thin jets that appear just beyond the mitral leaflets. However, the relation between jet size and MR severity presents a large range of variability because in addition to regurgitation severity, the colour flow display

Table 1 Probability of successful mitral valve repair in organic mitral regurgitation based on echo findings

Aetiology	Dysfunction	Calcification	Mitral annulus dilatation	Probability of repair
Degenerative	II: Localized prolapse (P2 and/or A2)	No/Localized	Mild/Moderate	Feasible
Ischaemic/Functional	I or IIIb	No	Moderate	Feasible
Barlow	II: Extensive prolapse (≥ 3 scallops, posterior commissure)	Localized (annulus)	Moderate	Difficult
Rheumatic	IIIa but pliable anterior leaflet	Localized	Moderate	Difficult
Severe Barlow	II: Extensive prolapse (≥ 3 scallops, anterior commissure)	Extensive (annulus + leaflets)	Severe	Unlikely
Endocarditis	II: Prolapse but destructive lesions	No	No/Mild	Unlikely
Rheumatic	IIIa but stiff anterior leaflet	Extensive (annulus + leaflets)	Moderate/Severe	Unlikely
Ischaemic/Functional	IIIb but severe valvular deformation	No	No or Severe	Unlikely

depends on many technical and haemodynamic factors. For a similar severity, patients with increased LA pressure or with eccentric jets that hug the LA wall or in whom the LA is enlarged may exhibit smaller jets area than those with normal LA pressure and size or with central jets (Figure 15).¹⁵ In acute MR, even centrally directed jets may be misleadingly small. Furthermore, as this method is a source of many errors, it is not recommended to assess MR severity. Nevertheless, the detection of a large eccentric jet adhering, swirling and reaching the posterior wall of the LA is in favour of significant MR. Conversely, small thin jets that appear just beyond the mitral leaflets usually indicate mild MR.

Key point

The colour flow area of the regurgitant jet is not recommended to quantify the severity of MR. The colour flow imaging should only be used for diagnosing MR.

Table 2 Unfavourable TTE characteristics for mitral valve repair in functional mitral regurgitation¹¹

Mitral valve deformation
Coaptation distance ≥ 1 cm
Tenting area $>2.5\text{--}3$ cm ²
Complex jets
Posterolateral angle $>45^\circ$
Local LV remodelling
Interpapillary muscle distance >20 mm
Posterior papillary-fibrosa distance >40 mm
Lateral wall motion abnormality
Global LV remodelling
EDD > 65 mm, ESD > 51 mm (ESV > 140 mL)
Systolic sphericity index >0.7

EDD, end-diastolic diameter; ESD, end-systolic diameter; ESV, end-systolic volume; LV, left ventricle.

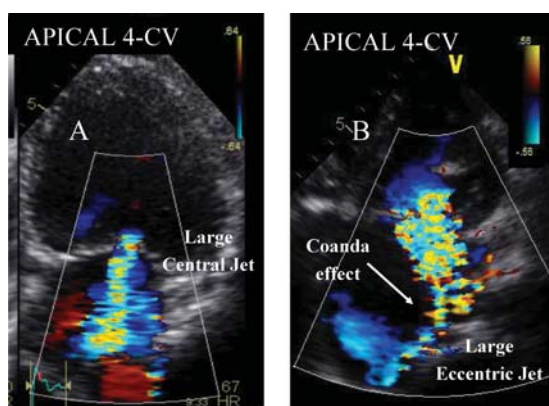


Figure 15 Visual assessment of mitral regurgitant jet using colour-flow imaging. Examples of two patients with severe mitral regurgitation. (A) Large central jet. (B) Large eccentric jet with a clear Coanda effect. CV, four-chamber view.

A more quantitative approach is required when more than a small central MR jet is observed.

Vena contracta width

The vena contracta is the area of the jet as it leaves the regurgitant orifice; it reflects thus the regurgitant orifice area.^{16–18} The vena contracta is typically imaged in a view perpendicular to the commissural line (e.g. the parasternal long-axis or the apical four-chamber view) using a careful probe angulation to optimize the flow image, an adapted Nyquist limit (colour Doppler scale) (40–70 cm/s) to perfectly identify the neck or narrowest portion of the jet and the narrowest Doppler colour sector scan coupled with the zoom mode to improve resolution and measurement accuracy (Figure 16). Averaging measurements over at least two to three beats and using two orthogonal planes whenever possible is recommended. A vena contracta <3 mm indicates mild MR whereas a width ≥ 7 mm defines severe MR. Intermediate values are not accurate at distinguishing moderate from mild or severe MR (large overlap); they require the use of another method for confirmation.

The concept of vena contracta is based on the assumption that the regurgitant orifice is almost circular. The orifice is roughly circular in organic MR; although in functional MR, it appears to be rather elongated along the mitral coaptation line and non-circular.^{19,20} Thus, the vena contracta could appear at the same time narrow in four-chamber view and broad in two-chamber view. Moreover, conventional 2D colour Doppler imaging does not provide appropriate orientation of 2D scan planes to obtain an accurate cross-sectional view of the vena contracta. The vena contracta can be classically well identified in both central and eccentric jets. In case of multiple MR jets, the respective widths of the vena contracta are not additive. Such characteristics may be better appreciated and measured on 3D echocardiography. In functional MR, a mean vena contracta width (four- and two-chamber views) has been shown to be better correlated with the 3D vena contracta. A mean value >8 mm on 2D echo (Figure 17) has been reported to define severe MR for all

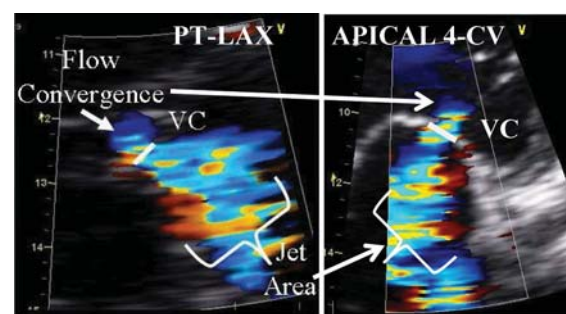


Figure 16 Semi-quantitative assessment of mitral regurgitation severity using the vena contracta width (VC). The three components of the regurgitant jet (flow convergence zone, vena contracta, jet turbulence) are obtained. CV, chamber view; PT-LAX, parasternal long-axis view.

aetiologies of MR including functional MR.^{21–23} These data need, however, to be confirmed in further studies.

Key point

When feasible, the measurement of vena contracta is recommended to quantify MR. Intermediate vena contracta values (3–7 mm) need confirmation by a more

quantitative method, when feasible. The vena contracta can often be obtained in eccentric jet. In case of multiple jets, the respective values of the vena contracta width are not additive. The assessment of the vena contracta by 3D echo is still reserved for research purposes.

The flow convergence method

Over the last few years, the flow convergence method has gained interest. It is now by far the most recommended quantitative approach whenever feasible.²⁴ The apical four-chamber view is classically recommended for optimal visualization of the proximal isovelocity surface area (PISA). However, the parasternal long- or short-axis view is often useful for visualization of the PISA in case of anterior mitral valve prolapse. The area of interest is optimized by lowering imaging depth and reducing the Nyquist limit to ~15–40 cm/s. The radius of the PISA is measured at mid-systole using the first aliasing. Regurgitant volume (R Vol) and effective regurgitant orifice area (EROA) are obtained using the standard formula (Figure 18). Qualitatively, the presence of flow convergence at a Nyquist limit of 50–60 cm/s should alert to the presence of significant MR. Grading of severity of organic MR classifies regurgitation as mild, moderate or severe, and sub-classifies the moderate regurgitation group into ‘mild-to-moderate’ (EROA of 20–29 mm² or a R Vol of 30–44 mL) and ‘moderate-to-severe’ (EROA of 30–39 mm² or a R Vol of 45–59 mL). Quantitatively, organic MR

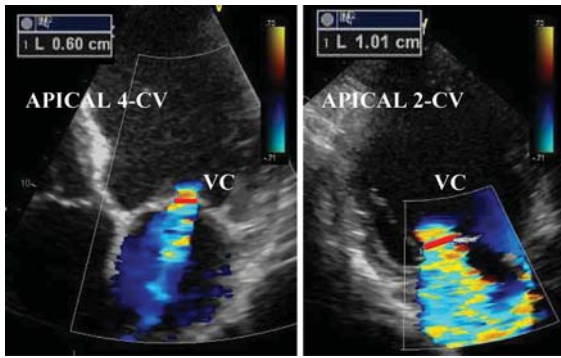


Figure 17 Semi-quantitative assessment of mitral regurgitation (MR) severity using the vena contracta width (VC) obtained from the apical four-chamber and two-chamber views (CV) in a patient with ischaemic functional MR. The mean vena contracta is calculated $[(6 + 10)/2 = 8 \text{ mm}]$.

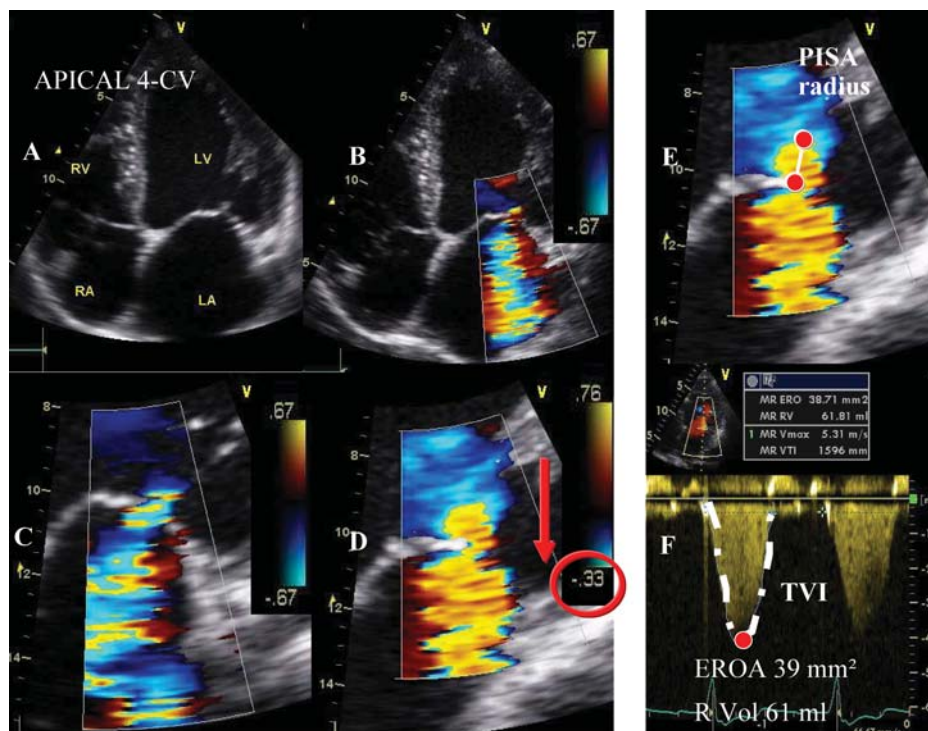


Figure 18 Quantitative assessment of mitral regurgitation (MR) severity using the proximal isovelocity surface area method. Stepwise analysis of MR: (A) Apical four-chamber view (CV); (B) colour-flow display; (C) zoom of the selected zone; (D) downward shift of zero baseline to obtain an hemispheric proximal isovelocity surface area; (E) measure of the proximal isovelocity surface area radius using the first aliasing; (F) continuous wave Doppler of MR jet allowing calculation the effective regurgitant orifice area (EROA) and regurgitant volume (R Vol). TVI, time-velocity integral.

is considered severe if EROA is $\geq 40 \text{ mm}^2$ and R Vol $\geq 60 \text{ mL}$. In ischaemic MR, the thresholds of severity, which are of prognostic value, are 20 mm^2 and 30 mL , respectively.²⁵ EROA is the most robust parameter as it represents a marker of lesion severity. A large EROA can lead to large regurgitant kinetic energy (large R Vol) but also to potential energy, with low R Vol but high LA pressure.

As mentioned in the first part of the EAE recommendations on the assessment of valvular regurgitation, the PISA method faces several advantages and limitations (Figures 19–21).^{1,26} Colour M-mode is important to assess the variation of the PISA during

systole (Figure 22). The PISA radius is most frequently constant in patients with rheumatic MR. It frequently increases progressively with a maximum during the second half of systole in patients with mitral valve prolapse. In the presence of functional MR, there is a dynamic variation of regurgitant orifice area with early and late systolic peaks and a mid-systolic decrease. These changes reflect the phasic variation in transmitral pressure that acts to close the mitral leaflets more effectively when pressure reaches its peak in mid-systole.²⁷ The PISA method is based on the assumption of hemispheric symmetry of the velocity distribution proximal to the regurgitant lesion, which may not hold for eccentric jets, multiple jets, or complex or elliptical regurgitant orifices. Practically, the geometry of the PISA varies, depending on the shape of the orifice and mitral valve leaflets surrounding the orifice. In functional MR, the PISA might look like an ellipsoidal shape and two separate MR jets originating from the medial and lateral sides of the coaptation line can be observed on 2D echo. When the shape of the flow convergence zone is not a hemisphere, the PISA method may underestimate the degree of functional MR, particularly when the ratio of long-axis length to short-axis length of the 3D regurgitant orifice is > 1.5 .²⁸ When the EROA is calculated with the hemispheric assumption (using the vertical PISA), the horizontal length of PISA is ignored. In organic MR, the shape of the PISA is rounder, which minimizes the risk of EROA underestimation (Figure 23). These findings could explain why the threshold used to define a severe functional MR is inferior to that used for organic MR. Careful consideration of the 3D geometry of PISA may be of interest in evaluating the severity of functional MR. The best 3D echo method to quantitate MR severity is still not defined.

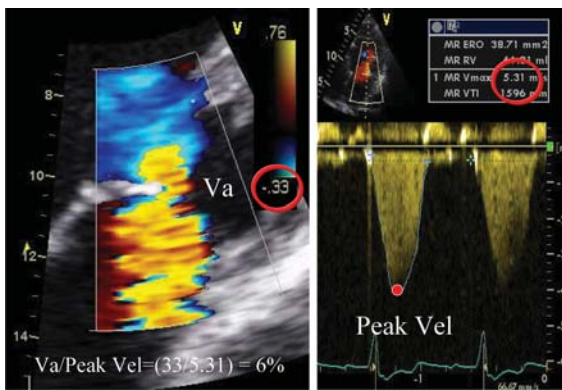


Figure 19 To avoid the underestimation of the regurgitant volume the ratio of the aliasing velocity (V_a) to peak orifice velocity (vel) is maintained $< 10\%$.

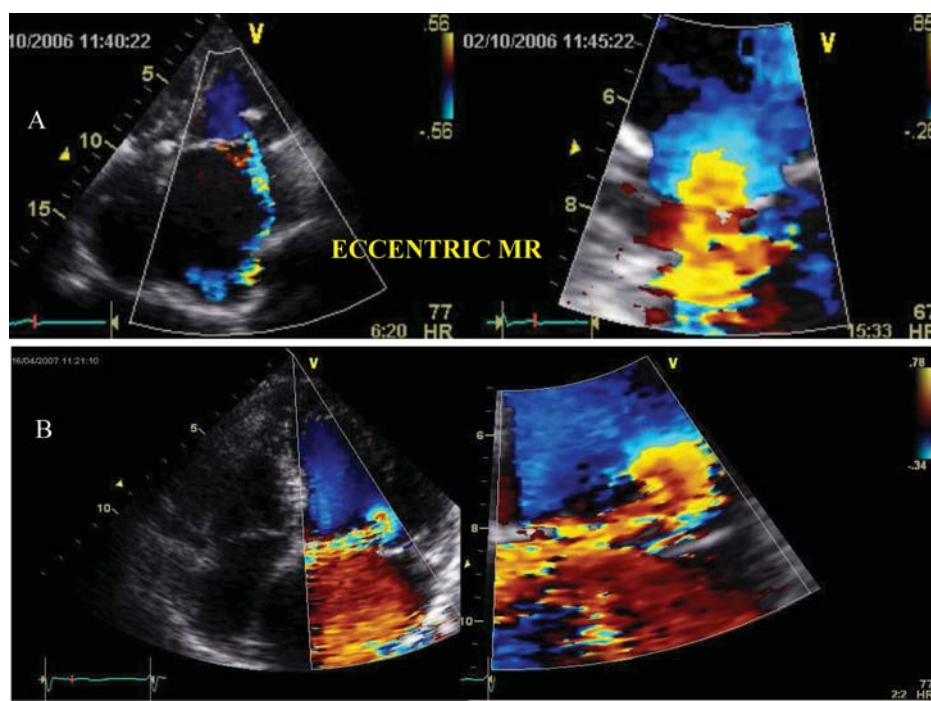


Figure 20 Example of eccentric mitral regurgitation that can still be perfectly assessed by using the proximal isovelocity surface area method.

Key point

When feasible, the PISA method is highly recommended to quantitate the severity of MR. It can be used in both central and eccentric jets. An EROA \geq

40 mm² or a R Vol \geq 60 mL indicates severe organic MR. In functional ischaemic MR, an EROA \geq 20 mm² or a R Vol \geq 30 mL identifies a subset of patients at increased risk of cardiovascular events.

Pulsed Doppler

Doppler volumetric method

Quantitative PW Doppler method can be used as an additive or alternative method, especially when the PISA and the vena contracta are not accurate or not applicable. This approach is time consuming and is associated with several drawbacks.^{1,29}

Key point

The Doppler volumetric method is a time-consuming approach that is not recommended as a first line method to quantify MR severity.

Anterograde velocity of mitral inflow: mitral to aortic time-velocity integral (TVI) ratio

In the absence of mitral stenosis, the increase in transmitral flow that occurs with increasing MR severity can be detected as higher flow velocities during early diastolic filling (increased E velocity). In the absence of mitral stenosis, a peak E velocity > 1.5 m/s suggests severe MR. Conversely, a dominant A wave (atrial contraction) basically excludes severe MR. These patterns are more applicable in patients older than 50 years old or in conditions of impaired myocardial relaxation. The pulsed Doppler mitral to aortic TVI ratio is also used as an easily measured index for the quantification of isolated pure organic MR. Mitral inflow Doppler tracings are obtained at the mitral leaflet tips and aortic flow at the annulus level in the apical four-chamber view. A TVI ratio

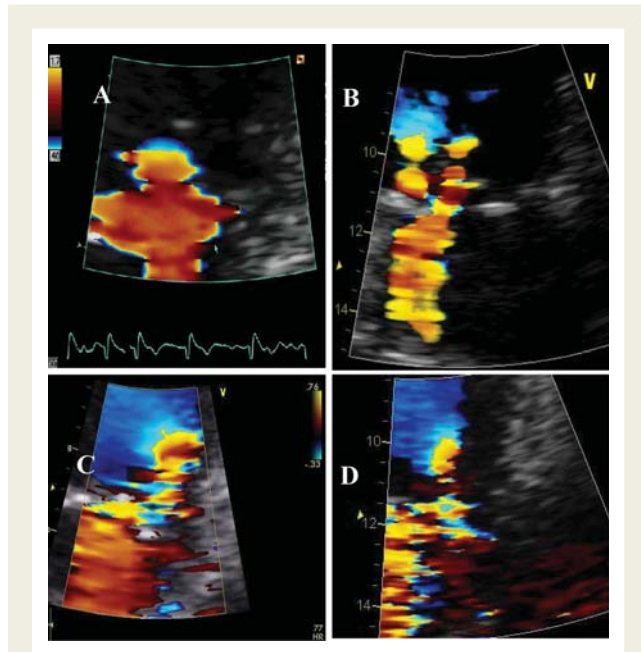


Figure 21 (A) Example of a flat flow convergence zone; (B) presence of two jets; (C and D) distorted and constrained flow convergence zone by the lateral myocardial wall.

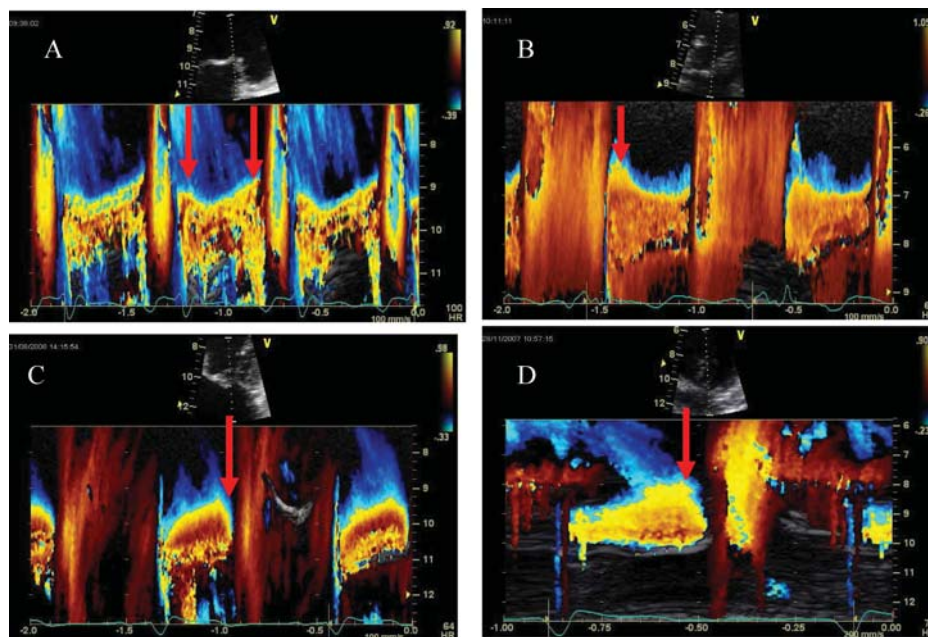


Figure 22 Four examples of flow convergence zone changes during systole using colour M-Mode. (A and B) Functional mitral regurgitation (A: early and late peaks and mid-systolic decreases; B: early systolic peak), (C) rheumatic mitral regurgitation with an end-systolic decrease in flow convergence zone, (D) M mitral valve prolapse (late systolic enhancement).

>1.4 strongly suggests severe MR whereas a TVI ratio <1 is in favour of mild MR (Figure 24).³⁰

Pulmonary venous flow

Pulsed Doppler evaluation of pulmonary venous flow pattern is another aid for grading the severity of MR (Figure 25).³¹

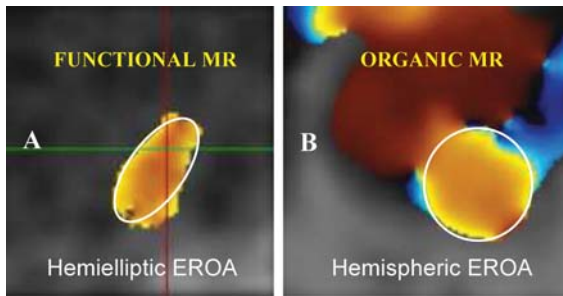


Figure 23 3D shape of the flow convergence in functional (A) (hemielliptic) and organic mitral regurgitation (B) (hemispheric).

In normal individuals, a positive systolic wave (S) followed by a smaller diastolic wave (D) is classically seen in the absence of diastolic dysfunction. With increasing severity of MR, there is a decrease of the S wave velocity. In severe MR, the S wave becomes frankly reversed if the jet is directed into the sampled vein. As unilateral pulmonary flow reversal can occur at the site of eccentric MR jets, sampling through all pulmonary veins is recommended, especially during transoesophageal echocardiography. Although, evaluation of right upper pulmonary flow can often be obtained using TTE, evaluation is best using TEE with the pulse Doppler sample placed about 1 cm deep into the pulmonary vein. Atrial fibrillation and elevated LA pressure from any cause can blunt forward systolic pulmonary vein flow. Therefore, blunting of pulmonary venous flow lacks of specificity for the diagnosis of severe MR.

Key point

Both the pulsed Doppler mitral to aortic TVI ratio and the systolic pulmonary flow reversal are specific for severe MR. They represent the strongest additional parameters for evaluating MR severity.

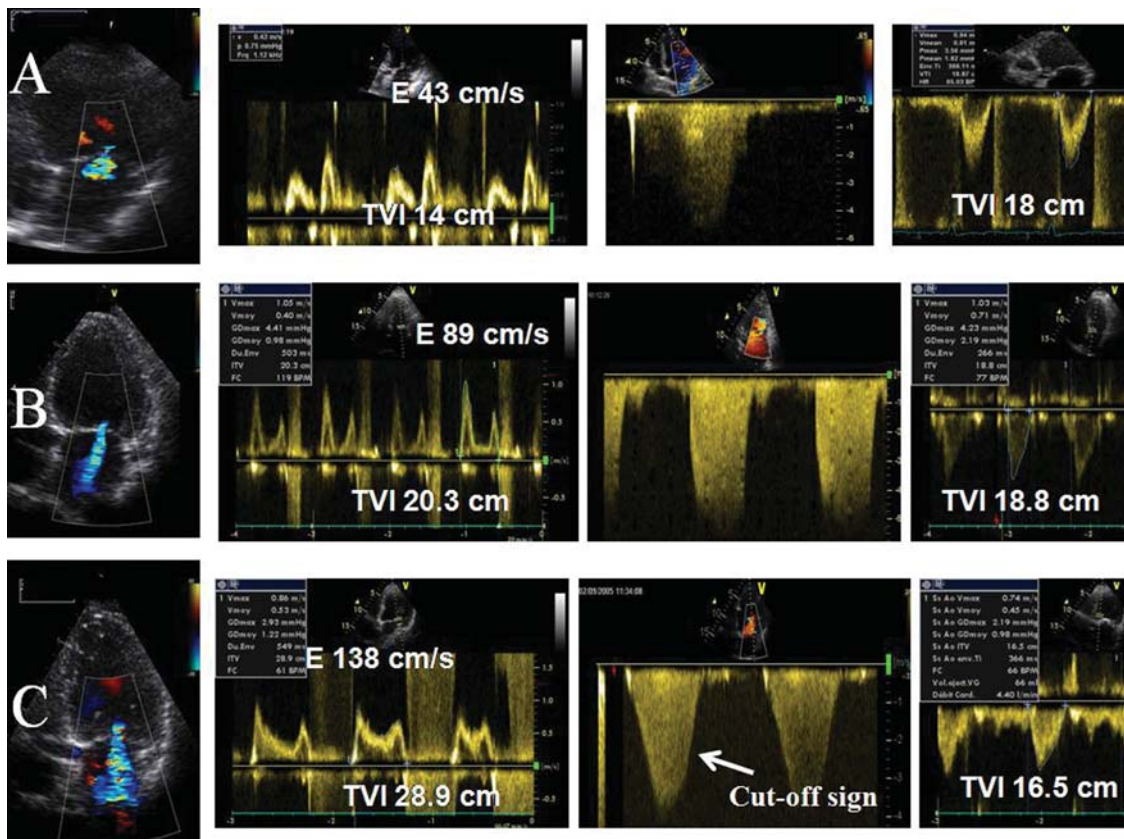


Figure 24 Three examples of various degrees of mitral regurgitation (MR), mild (A), moderate (B), and severe (C) are provided. The regurgitant jet as well as the mitral E wave velocity increase with the severity of MR. In severe MR, the continuous wave Doppler signal of the regurgitant jet is truncated, triangular and intense. Notching of the continuous wave envelope (cut-off sign) can occur in severe MR. TVI, time-velocity integral.

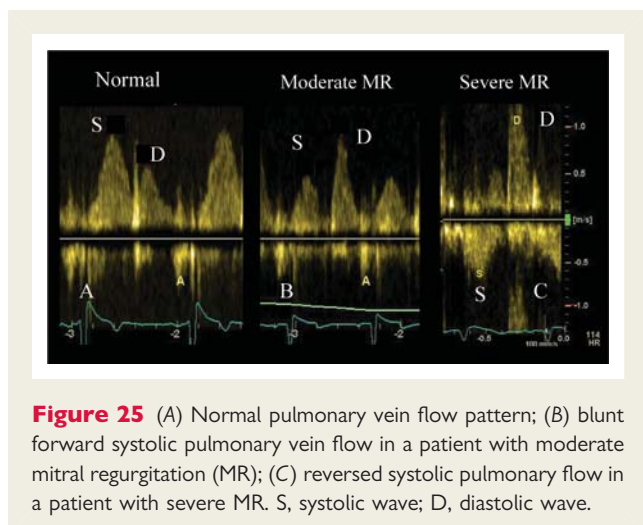


Figure 25 (A) Normal pulmonary vein flow pattern; (B) blunt forward systolic pulmonary vein flow in a patient with moderate mitral regurgitation (MR); (C) reversed systolic pulmonary flow in a patient with severe MR. S, systolic wave; D, diastolic wave.

Continuous wave Doppler of mitral regurgitation jet

Peak MR jet velocities by CW Doppler typically range between 4 and 6 m/s. This reflects the high systolic pressure gradient between the LV and LA. The velocity itself does not provide useful information about the severity of MR. Conversely, the signal intensity (jet density) of the CW envelope of the MR jet can be a qualitative guide to MR severity. A dense MR signal with a full envelope indicates more severe MR than a faint signal. The CW Doppler envelope may be truncated (notch) with a triangular contour and an early peak velocity (blunt). This indicates elevated LA pressure or a prominent regurgitant pressure wave in the LA due to severe MR. In eccentric MR, it may be difficult to record the full CW envelope of the jet because of its eccentricity, while the signal intensity shows dense features.

Key point

The CW Doppler density of the MR jet is a qualitative parameter of MR severity.

Consequences of mitral regurgitation

The presence of severe MR has significant haemodynamic effects, primarily on the LV and LA.

Left ventricle size and function

The LV dimensions and ejection fraction reflect the heart's ability to adapt to increased volume load. In the chronic compensated phase (the patient could be asymptomatic), the forward stroke volume is maintained through an increase in LV ejection fraction. Such patients typically have LV ejection fraction $>65\%$. Even in the acute stage, the LV ejection fraction increase in response to the increased preload. In the chronic decompensated phase (the patient could still be asymptomatic or may fail to recognize deterioration in clinical status), the forward stroke volume decreases and the LA pressure increases significantly. The LV contractility can thus decrease silently and irreversibly. However, the LV ejection fraction may still be in the low normal range despite the presence of significant muscle dysfunction. In the current guidelines, surgery is recommended in asymptomatic patients with severe organic MR when the LV ejection fraction is $\leq 60\%$. The end-systolic diameter is less preload dependent than

the ejection fraction and could in some cases be more appropriate to monitor global LV function. An end-systolic diameter >45 mm (or ≥ 40 mm or >22 mm/m², AHA/ACC), also indicates the need for mitral valve surgery in these patients.^{2,32,33} New parameters are currently available for a better assessment of LV function. A systolic tissue Doppler velocity measured at the lateral annulus <10.5 cm/s has been shown to identify subclinical LV dysfunction and to predict post-operative LV dysfunction in patients with asymptomatic organic MR.³⁴ Strain imaging allows a more accurate estimation of myocardial contractility than tissue Doppler velocities. It is not influenced by translation or pathologic tethering to adjacent myocardial segments, which affect myocardial velocity measurements. In MR, strain has been shown to decrease even before LV end-systolic diameter exceeds 45 mm.³⁵ A resting longitudinal strain rate value $<1.07/s$ (average of 12 basal and mid segments) is associated with the absence of contractile reserve during exercise and thus with subclinical latent LV dysfunction.³⁶ By using the 2D-speckle tracking imaging (an angle independent method), a global longitudinal strain $<18.1\%$ has been associated with post-operative LV dysfunction.³⁷ Practically, the incremental value of tissue Doppler and strain imaging for identifying latent LV dysfunction remains to be determined.

Left atrial size and pulmonary pressures

The LA dilates in response to chronic volume and pressure overload. A normal sized LA is not normally associated with significant MR unless it is acute, in which case the valve appearance is likely to be grossly abnormal. LA remodelling (diameter >40 – 50 mm or LA volume index >40 mL/m²) may predict onset of atrial fibrillation and poor prognosis in patients with organic MR.³⁸ Conversely, MV repair leads to LA reverse remodelling, the extent of which is related to pre-operative LA size and to procedural success.³⁹ The excess regurgitant blood entering in the LA may induce acutely or chronically a progressive rise in pulmonary pressure. The presence of TR even if it is mild, permits the estimation of systolic pulmonary arterial pressure. Recommendation for mitral valve repair is a class IIa when pulmonary arterial systolic pressure is >50 mm Hg at rest.

Key point

When MR is more than mild MR, providing the LV diameters, volumes and ejection fraction as well as the LA dimensions (preferably LA volume) and the pulmonary arterial systolic pressure in the final echocardiographic report is mandatory.¹ The assessment of regional myocardial function (systolic myocardial velocities, strain, strain rate) is reasonable particularly in asymptomatic patients with severe organic MR and borderline values in terms of LV ejection fraction (60–65%) or LV end-systolic diameter (closed to 40 mm or 22 mm/m²).

Role of exercise echocardiography

Organic mitral regurgitation

In asymptomatic patients with severe MR, exercise stress echocardiography may help identify patients with unrecognized symptoms or subclinical latent LV dysfunction. Moreover, exercise echocardiography may also be helpful in patients with equivocal symptoms out of proportion of MR severity at rest. Worsening of MR severity, a marked increase in pulmonary arterial pressure, impaired exercise

capacity, and the occurrence of symptoms during exercise echocardiography can be useful findings to identify a subset of patients at higher risk who may benefit from early surgery.⁴⁰ A pulmonary artery systolic pressure >60 mmHg during exercise has been suggested as a threshold value above which asymptomatic patients with severe MR might be referred for surgical valve repair. Although the inclusion of pulmonary hypertension as an indication for valve surgery in the guidelines seems logical from a pathophysiological standpoint, there are, surprisingly, very limited outcome data to support this recommendation as well as the selected cut-off value for pulmonary arterial pressure (>60 mmHg, ACC/AHA). The application of stress echocardiography in organic MR is rated as a class IIa recommendation with level of evidence C in the ACC/AHA guidelines. To note, the place of stress echocardiography in this setting is not defined in the ESC recommendations, probably because of lack of robust data. An inability to increase the LV ejection fraction ($<4\%$) or reduce the end-systolic volume after treadmill exercise has been shown to reflect the presence of an impaired contractile reserve, and to be reliable early markers for progressive deterioration in myocardial contractility.³⁶ The absence of contractile reserve has also been associated with post-operative morbidity. A small change in 2D-speckle global longitudinal strain at exercise ($<1.9\%$) has also been correlated with post-operative LV dysfunction. The incremental value of these cut-off values remains to be confirmed.³⁷

Key point

Exercise echocardiography is useful in asymptomatic patients with severe organic MR and borderline values of LV ejection fraction (60–65%) or LV end-systolic diameter (closed to 40 mm or 22 mm/m²). The absence of contractile reserve could identify patients at increased risk of cardiovascular events. Moreover, exercise echocardiography may also be helpful in patients with equivocal symptoms out of proportion of MR severity at rest.

Functional mitral regurgitation

Quantitation of functional MR during exercise is feasible using the PISA method.⁴¹ The degree of MR at rest is unrelated to exercise-induced changes in ERO.⁸ Dynamic MR is strongly related to exercise-induced changes in systolic tenting area and to intermittent changes in LV synchronicity. Large exercise-induced increases in functional ischaemic MR (EROA ≥ 13 mm²) are associated with dyspnea or acute pulmonary oedema.^{42,43} Dynamic MR also predicts mortality and hospitalization for heart failure. Exercise stress echocardiography may thus unmask haemodynamically significant MR in patients with functional ischaemic LV systolic dysfunction and only mild to moderate MR at rest, and in doing so identify patients at higher risk for heart failure and death. Exercise Doppler echocardiography might provide useful information in the following patients with ischaemic MR: (i) those with exertional dyspnea out of proportion to the severity of resting LV dysfunction or MR; (ii) those in whom acute pulmonary edema occurs without an obvious cause; and (iii) those with moderate MR before surgical revascularization.

Key point

Exercise echocardiography is useful in patients with functional ischaemic MR and chronic LV systolic dysfunction to unmask the dynamic behaviour of MR. Patients

with an increase in EROA by ≥ 13 mm² are patients at increased risk of cardiovascular events. In these patients, exercise echocardiography also helps to identify the presence and extent of viable myocardium at jeopardy.

Integrating indices of severity

Echocardiographic assessment of MR includes integration of data from 2D/3D imaging of the valve and ventricle as well as Doppler measures of regurgitation severity (Table 3). Effort should be made to quantify the degree of regurgitation, except in the presence of mild or less MR. Both the vena contracta width and the PISA method are recommended. Adjunctive parameters help to consolidate about the severity of MR and should be widely used particularly when there is discordance between the quantified degree of MR and the clinical context. For instance, a modest regurgitant volume reflects severe MR when it develops acutely into a small, non-compliant LA and it may cause pulmonary congestion and systemic hypotension. Advantages and limitations of the various echo Doppler parameters used in assessing MR severity are detailed in Table 4.

Recommended follow-up

Moderate organic MR requires clinical examination every year and an echocardiogram every 2 years. In patients with severe organic MR, clinical assessment is needed every 6 months and an echocardiogram every 1 year. If the ejection fraction is 60–65% and/or if end-systolic diameter is closed to 40 or 22 mm/m², the echocardiogram should be performed every 6 months.¹ Progression of MR severity is frequent with important individual differences. The average yearly increase in regurgitant volume is 7.5 mL and 5.9 mm² in EROA.⁴⁴ In addition, the progression of other parameters need to be assessed: the increase in annular size, the development of a flail leaflet, the evolution of LV end-systolic dimension, LV ejection fraction, LA area or volume, pulmonary systolic arterial pressure, exercise capacity, and occurrence of atrial arrhythmias.

Tricuspid regurgitation

TR is a common insufficiency. Since it is mostly asymptomatic and not easily audible on physical examination, it is frequently only diagnosed by echocardiography performed for another indication. Although a mild degree of TR is frequent and benign, moderate and severe TR are associated with poor prognosis.

Anatomy and function of the tricuspid valve

The tricuspid valve complex is similar to the mitral valve but has greater variability. It consists of the annulus, leaflets, right ventricle (RV), papillary muscles, and chordae tendineae. The tricuspid valve lays between the right atrium (RA) and the RV and is placed in a slightly more apical position than the mitral valve.⁴⁵

The tricuspid valve has three leaflets of unequal size: the anterior leaflet is usually the largest and extends from the infundibula region anteriorly to the inferolateral wall posteriorly; the septal leaflet extends from the interventricular septum to the

Table 3 Grading the severity of organic mitral regurgitation

Parameters	Mild	Moderate	Severe
Qualitative			
MV morphology	Normal/Abnormal	Normal/Abnormal	Flail leaflet/Ruptured PMs
Colour flow MR jet	Small, central	Intermediate	Very large central jet or eccentric jet adhering, swirling and reaching the posterior wall of the LA
Flow convergence zone ^a	No or small	Intermediate	Large
CW signal of MR jet	Faint/Parabolic	Dense/Parabolic	Dense/Triangular
Semi-quantitative			
VC width (mm)	<3	Intermediate	≥7 (>8 for biplane) ^b
Pulmonary vein flow	Systolic dominance	Systolic blunting	Systolic flow reversal ^c
Mitral inflow	A wave dominant ^d	Variable	E wave dominant (>1.5 cm/s) ^e
TVI mit /TVI Ao	<1	Intermediate	>1.4
Quantitative			
EROA (mm ²)	<20	20–29; 30–39 ^f	≥40
R Vol (mL)	<30	30–44; 45–59 ^f	≥60
+ LV and LA size and the systolic pulmonary pressure ^g			

CW, continuous-wave; LA, left atrium; EROA, effective regurgitant orifice area; LV, left ventricle; MR, mitral regurgitation; R Vol, regurgitant volume; VC, vena contracta.

^aAt a Nyquist limit of 50–60 cm/s

^bFor average between apical four- and two-chamber views.

^cUnless other reasons of systolic blunting (atrial fibrillation, elevated LA pressure).

^dUsually after 50 years of age;

^eIn the absence of other causes of elevated LA pressure and of mitral stenosis.

^fGrading of severity of organic MR classifies regurgitation as mild, moderate or severe, and sub-classifies the moderate regurgitation group into 'mild-to-moderate' (EROA of 20–29 mm² or a R Vol of 30–44 mL) and 'moderate-to-severe' (EROA of 30–39 mm² or a R Vol of 45–59 mL).

^gUnless for other reasons, the LA and LV size and the pulmonary pressure are usually normal in patients with mild MR. In acute severe MR, the pulmonary pressures are usually elevated while the LV size is still often normal. In chronic severe MR, the LV is classically dilated. Accepted cut-off values for non significant left-sided chambers enlargement: LA volume <36 mL/m², LV end-diastolic diameter <56 mm, LV end-diastolic volume <82 mL/m², LV end-systolic diameter <40 mm, LV end-systolic volume <30 mL/m², LA diameter <39 mm, LA volume <29 mL/m².

posterior ventricular border; the posterior leaflet attaches along the posterior margin of the annulus from the septum to the inferolateral wall. The insertion of the septal leaflet of the tricuspid valve is characteristically apical relative to the septal insertion of the anterior mitral leaflet. The three main TTE views allowing the tricuspid valve visualization are the parasternal, the apical four-chamber and the subcostal views. Parasternal long-axis view of the RV inflow is obtained by tilting the probe inferomedially and rotating it slightly clockwise from the parasternal long-axis view of the LV. This incidence reveals the anterior tricuspid leaflet (near the aortic valve) and the posterior tricuspid leaflet. Parasternal short-axis view, at the level of the aortic valve, apical four-chamber view and subcostal four-chamber view visualize the septal and the anterior tricuspid leaflets (Figure 26). TEE for the tricuspid valve is possible with the four-chamber view at 0° in the basal transoesophageal and oesogastric junction planes. TEE is of interest for the diagnosis of endocarditis when suspected. It is particularly essential to diagnose venous catheters and pacemakers lead infection because TTE is often non diagnostic in these settings. TEE can also help accurate tricuspid valve chordae visualization when traumatic rupture is suspected with TTE. However, it is rarely possible to visualize by 2D echo the three leaflets simultaneously. Real-time 3D TTE is now routinely available and allows, with its unique capability of obtaining a short-axis plane of the tricuspid valve, simultaneous visualization of the three leaflets moving during the cardiac cycle and their attachment to the tricuspid annulus.⁴⁶ 3D

echo supplements 2D echo and TEE with detailed images of the morphology of the valve including leaflets size and thickness, annulus shape and size, myocardial walls, and their anatomic relationships.

The tricuspid annulus, providing a firm support for the tricuspid leaflets insertion, is slightly larger than the mitral valve annulus. The tricuspid annulus shows a non-planar structure with an elliptical saddle-shaped pattern, having two high points (oriented superiorly towards the RA) and two low points (oriented inferiorly toward the RV that is best seen in mid-systole). Normal tricuspid valve annulus diameter in adults is 28 ± 5 mm in the four-chamber view. Significant tricuspid annular dilatation is defined by a diastolic diameter of >21 mm/m² (>35 mm). A correlation exists between tricuspid annulus diameter and TR severity: a systolic tricuspid annulus diameter >3.2 cm or a diastolic tricuspid annulus diameter >3.4 cm are often markers in favour of more significant TR. The normal motion and contraction of the tricuspid annulus also contributes to maintaining valve competence. The normal contraction (decrease in annular area in systole) of the tricuspid annulus is 25%. These reference measures are currently used to propose tricuspid valve repair at the time of left-sided valve surgery. However, as the shape of the tricuspid annulus is not circular but oval, with a minor and a major diameter, the 2D echo measurement of the tricuspid annulus diameters (apical four-chamber view, parasternal short-axis view) systematically underestimate the actual tricuspid annulus size by 3D echo. As a consequence, 65% of patients

Table 4 Echocardiographic parameters used to quantify mitral regurgitation severity: recordings, advantages and limitations

Parameters	Recordings	Usefulness/advantages	Limitations
Mitral valve morphology	<ul style="list-style-type: none"> • Visual assessment • Multiple views 	<ul style="list-style-type: none"> • Flail valve or ruptured PMs are specific for significant MR 	<ul style="list-style-type: none"> • Other abnormalities are non-specific of significant MR
Colour flow MR jet	<ul style="list-style-type: none"> • Optimize colour gain/scale • Evaluate in two views • Need blood pressure evaluation 	<ul style="list-style-type: none"> • Ease of use • Evaluates the spatial orientation of MR jet • Good screening test for mild vs. severe MR 	<ul style="list-style-type: none"> • Can be inaccurate for estimation of MR severity • Influenced by technical and haemodynamic factors • Underestimates eccentric jet adhering the LA wall (Coanda effect)
VC width	<ul style="list-style-type: none"> • Two orthogonal planes (PT-LAX, AP-4CV) • Optimize colour gain/scale • Identify the three components of the regurgitant jet (VC, PISA, Jet into LA) • Reduce the colour sector size and imaging depth to maximize frame rate • Expand the selected zone (Zoom) • Use the cine-loop to find the best frame for measurement • Measure the smallest VC (immediately distal to the regurgitant orifice, perpendicular to the direction of the jet) 	<ul style="list-style-type: none"> • Relatively quick and easy • Relatively independent of haemodynamic and instrumentation factors • Not affected by other valve leak • Good for extremes MR: mild vs. severe • Can be used in eccentric jet 	<ul style="list-style-type: none"> • Not valid for multiple jets • Small values; small measurement errors leads to large % error • Intermediate values need confirmation • Affected by systolic changes in regurgitant flow
PISA method	<ul style="list-style-type: none"> • Apical four-chamber • Optimize colour flow imaging of MR • Zoom the image of the regurgitant mitral valve • Decrease the Nyquist limit (colour flow zero baseline) • With the cine mode select the best PISA • Display the colour off and on to visualize the MR orifice • Measure the PISA radius at mid-systole using the first aliasing and along the direction of the ultrasound beam • Measure MR peak velocity and TVI (CW) • Calculate flow rate, EROA, R Vol 	<ul style="list-style-type: none"> • Can be used in eccentric jet • Not affected by the aetiology of MR or other valve leak • Quantitative: estimate lesion severity (EROA) and volume overload (R Vol) • Flow convergence at 50 cm/s alerts to significant MR 	<ul style="list-style-type: none"> • PISA shape affected <ul style="list-style-type: none"> – by the aliasing velocity – in case of non-circular orifice – by systolic changes in regurgitant flow – by adjacent structures (flow constraintment) • PISA is more a hemi-ellipse • Errors in PISA radius measurement are squared • Inter-observer variability • Not valid for multiple jets
Doppler volumetric method (PW)	<p>Flow across the mitral valve</p> <ul style="list-style-type: none"> • Measure the mitral inflow by placing the PW sample volume at the mitral annulus (AP-4CV) • Measure the mitral annulus diameter (AP-4CV) at the maximal opening of the mitral valve (two to three frames after the end-systole). <p>Flow across the aortic valve</p> <ul style="list-style-type: none"> • Measure the LV outflow tract flow by placing the PW sample volume 5 mm below the aortic cusps (AP-5CV) • Measure the LV outflow tract diameter (parasternal long-axis view) 	<ul style="list-style-type: none"> • Quantitative: estimate lesion severity (ERO) and volume overload (R Vol) • Valid in multiple jets 	<ul style="list-style-type: none"> • Time consuming • Requires multiple measurements: source of errors • Not applicable in case of significant AR (use the pulmonic site) • Difficulties in assessing mitral annulus diameter and mitral inflow in case of calcific mitral valve/annulus • Affected by sample volume location (mitral inflow)

Continued

Table 4 Continued

Parameters	Recordings	Usefulness/advantages	Limitations
CW MR jet profile	<ul style="list-style-type: none"> Apical four-chamber 	<ul style="list-style-type: none"> Simple, easily available 	<ul style="list-style-type: none"> Qualitative, Complementary finding Complete signal difficult to obtain in eccentric jet
Pulmonary vein flow	<ul style="list-style-type: none"> Apical four-chamber Sample volume of PW places into the pulmonary vein Interrogate the different pulmonary veins when possible 	<ul style="list-style-type: none"> Simple Systolic flow reversal is specific for severe MR 	<ul style="list-style-type: none"> Affected by LA pressure, atrial fibrillation Not accurate if MR jet directed into sampled vein
Peak E velocity	<ul style="list-style-type: none"> Apical four-chamber Sample volume of PW places at mitral leaflet tips 	<ul style="list-style-type: none"> Simple, easily available Dominant A-wave almost excludes severe MR 	<ul style="list-style-type: none"> Affected by LA pressure, atrial fibrillation, LV relaxation Complementary finding
Atrial and LV size	<ul style="list-style-type: none"> Use preferably the Simpson method 	<ul style="list-style-type: none"> Dilatation sensitive for chronic significant MR Normal size almost excludes significant chronic MR 	<ul style="list-style-type: none"> Dilatation observed in other conditions (non specific) May be normal in acute severe MR

CW, continuous-wave; LA, left atrium; EROA, effective regurgitant orifice area; LV, left ventricle; MR, mitral regurgitation; PW, pulse wave; R Vol, regurgitant volume; VC, vena contracta.

with normal tricuspid annulus diameter at 2D echo show grade 1–2 TR compared with 30% of patients with normal tricuspid annulus size at 3D echo.^{47,48} Conversely, calculation of tricuspid annulus fractional shortening yields the same results using 2D echo and 3D echo since the extent of underestimation of tricuspid annulus diameter made by 2DE is comparable in diastole and in systole.

Three papillary muscle groups (anterior, posterior, and septal) usually support the TV leaflets and lie beneath each of the three commissures. The papillary muscles exhibit variability in size. The anterior and septal papillary muscles are the largest. The posterior papillary muscle is small and, at times, absent. The anterior papillary muscle has attachments to the moderator band. Each leaflet has chordal attachments to one or more papillary muscles.

Aetiology and mechanisms

Small physiologic degrees of TR are frequently encountered in the normal disease-free individual. The prevalence could reach 65–75%.⁴⁹ On echocardiography, this 'physiological' TR is associated with normal valve leaflets and no dilatation of the RV. It is localized in a small region adjacent to valve closure (<1 cm), with a thin central jet and often does not extend throughout systole. Peak systolic velocities are between 1.7 and 2.3 m/s.

In the pathologic situation, a complete understanding of leaflet morphology and of the pathophysiological mechanisms underlying TR could potentially lead to improved techniques for valve repair and to design physiologically suitable annular rings. It should be stressed that TR is most often seen in patients with multiple valvular disease especially aortic or mitral valve disease. The most common cause of TR is not a primary tricuspid valve disease (organic TR) but rather an impaired valve coaptation (secondary or functional TR) caused by dilation of the RV and/or of the

tricuspid annulus. A variety of primary disease processes can affect the tricuspid valve complex directly and lead to valve incompetence: infective endocarditis, congenital disease like Ebstein anomaly or atrioventricular canal, rheumatic fever, carcinoid syndrome, endomyocardial fibrosis, myxomatous degeneration of the tricuspid valve leading to prolapse, penetrating and non-penetrating trauma, and iatrogenic damages during cardiac surgery, biopsies, and catheter placement in right heart chambers.

Aetiology

Degenerative tricuspid regurgitation

As for MR, three types of tricuspid changes can be visualized: a billowing valve, a prolapsing valve and a flail tricuspid valve. Tricuspid prolapse is generally associated with mitral valve prolapse and is defined as a mid-systole posterior leaflet displacement beyond the annular plane. The coaptation line is behind the annular plane. Tricuspid prolapse most often involves the septal and anterior tricuspid leaflets. The most common phenotype of tricuspid prolapse is diffuse myxomatous degeneration (Barlow's disease). A flail tricuspid leaflet is observed when the free edge of a leaflet is completely reversed in the RA, usually as a consequence of ruptured chordae (degenerative TR, infective endocarditis, trauma).

Rheumatic tricuspid regurgitation

Rheumatic involvement of the tricuspid valve is less common than that of left-sided valves. Regurgitation is a consequence of deformity, shortening and retraction of one or more leaflets of the tricuspid valve as well as shortening and fusion of the chordae tendineae and papillary muscles. 2D echo usually detects thickening and the distortion of the leaflets but cannot provide a comprehensive assessment of extension of valve apparatus involvement. The 3D full-volume data set from apical approach usually provides a

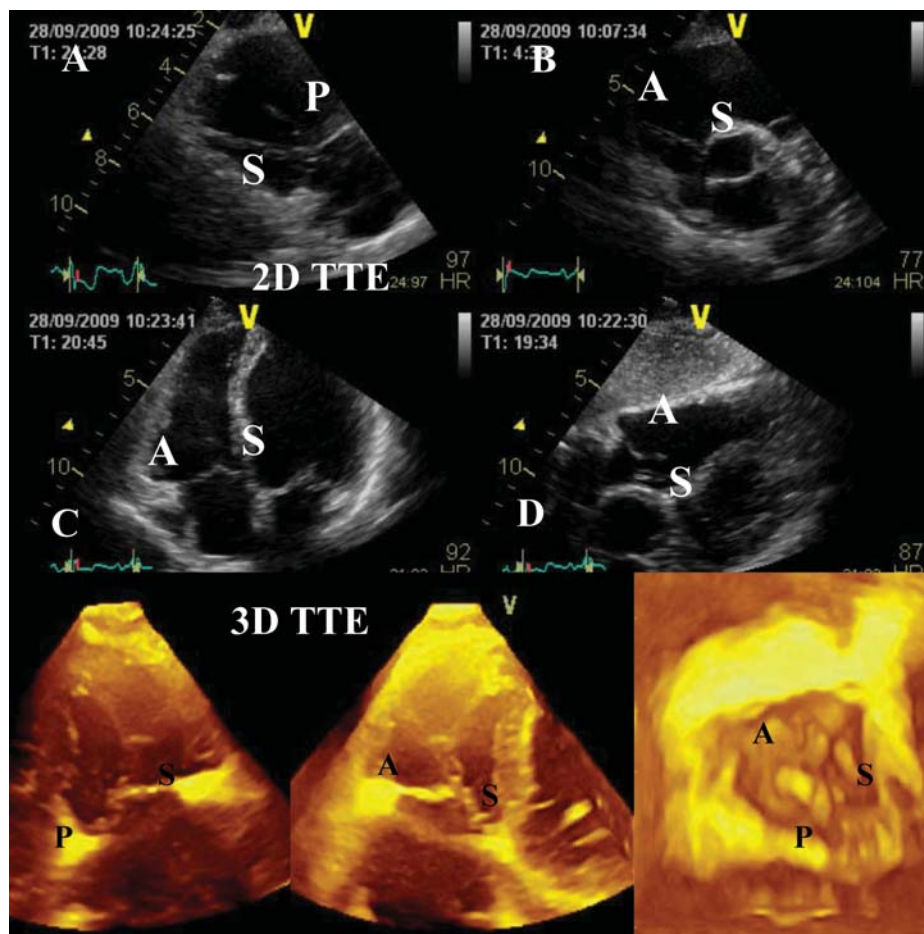


Figure 26 2D and 3D echo recordings of the tricuspid valve. (A) Parasternal long-axis view; (B) parasternal short-axis view at the level of the aortic valve; (C) apical four-chamber view; (D) sub-costal view. A, anterior leaflet; S, septal leaflet; P, posterior leaflet.

comprehensive assessment of the whole tricuspid valve apparatus which can be examined from different perspectives. The 'en face' view of the tricuspid valve obtained by 3D echo allows the visualization of the commissural fusion.

Functional tricuspid regurgitation

Functional TR results from the adverse effects on RV function and geometry caused by left-sided heart valve diseases, pulmonary hypertension, congenital heart defects, and cardiomyopathy. The progressive remodelling of the RV volume leads to tricuspid annular dilatation, papillary muscle displacement and tethering of the leaflets, resulting in TR. TR itself leads to further RV dilation and dysfunction, more tricuspid annular dilatation and tethering, and worsening TR. With increasing TR the RV dilates and eventually fails, causing increased RV diastolic pressure and, in advanced situations a shift of the interventricular septum toward the LV. Such ventricular interdependence might reduce the LV cavity size (pure compression), causing restricted LV filling and increased LV diastolic and pulmonary artery pressure. The tricuspid annular dilatation, the lost of its contraction and the increased tethering are probably the most important factors in the development of TR. Indeed, the

tricuspid annulus is not saddle-shaped anymore; it becomes flat, planar, and distorted. Increased tethering (apical displacement of the tricuspid leaflets) can be evaluated by the measurement of the systolic tenting area (area between the tricuspid annulus and the tricuspid leaflets body) and the coaptation distance (distance between the tricuspid annular plane and the point of coaptation) in mid-systole from the apical four-chamber view. A tenting area $>1 \text{ cm}^2$ has been shown to be associated with severe TR.⁵⁰

Carcinoid tricuspid regurgitation

In the carcinoid disease, the valve appears thickened, fibrotic with markedly restricted motion during cardiac cycle. Both 2D/3D echo can show the regions of ineffective leaflet coaptation and the lack of commissural fusion.

Mechanism

In recent years, repair techniques for diseased tricuspid valves have evolved. Precise determination of the mechanisms of TR has thus become an essential component of the echocardiographic examination (Figure 27). The Carpentier's classification remains the most common used functional classification: type I:

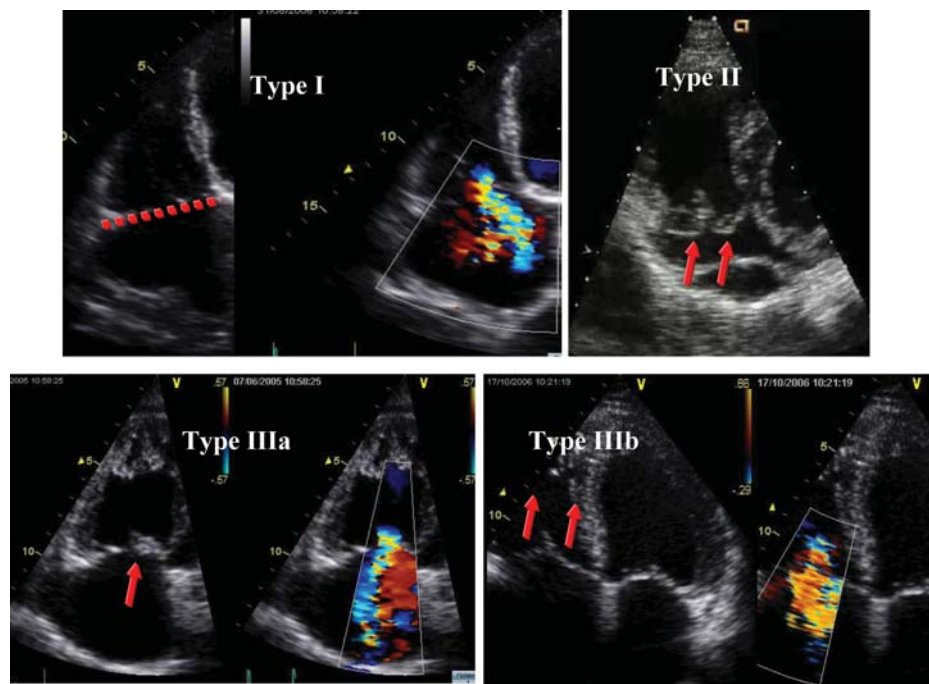


Figure 27 Mechanisms of mitral regurgitation according to the Capentier's functional classification.

leaflet perforation (infective endocarditis) or more frequently by annular dilatation; type II: prolapse of one or more leaflets (tricuspid valve prolapse); and type III: restricted motion as the consequence of rheumatic disease, significant calcifications, toxic valvulopathy, functional TR.

Persistent or recurrent TR has been reported in up to 20–50% of patients undergoing mitral valve surgery.⁵¹ In functional TR, this has been related to the extent of tricuspid leaflet restriction and to the severity of tricuspid annular dilatation. Both the severity of pre-operative TR and RV dysfunction contributes to residual post-operative TR. Similarly, severe tricuspid valve tethering predicts residual TR after tricuspid valve annuloplasty. A tenting area $>1.63 \text{ cm}^2$ and a tethering distance $>0.76 \text{ cm}$ are good predictors of residual TR after tricuspid valve surgery.⁵²

Key point

In the presence of TR, tricuspid valve analysis is mandatory. 2D-TTE imaging is the technique of choice. 3D-TTE can be used as an additive approach. TEE is advised in case of suboptimal TTE images. Distinction between primary and secondary TR is warranted.

Assessment of tricuspid regurgitation severity

Colour flow Doppler

Grading the severity of TR is in principle similar to MR. However, because standards for determining the TR severity are less robust than for MR, the algorithms for relating colour flow derived parameters to TR severity are less well developed.

Colour flow imaging

Colour-flow imaging is useful to recognize small jets, but the assessment of larger TR jets has important limitations.⁵³ Indeed, flow jets that are directed centrally into the RA generally appear larger than eccentric wall-impinging jets with similar or worse severity. Basically, multiple windows (apical four-chamber, parasternal long and short axis views, sub-costal view) are recommended to assess TR severity by colour-flow analysis (Figure 28). The general assumption is that larger colour jets that extend deep into the RA represent more TR than small thin jets that appear just beyond the tricuspid leaflets. As for MR, this method is a source of many errors and is limited by several technical and haemodynamic factors. Furthermore, it is not recommended to assess TR severity. Nevertheless, the detection of a large eccentric jet adhering, swirling and reaching the posterior wall of the RA is in favour of significant TR. Conversely, small thin central jets usually indicate mild TR.

Key point

The colour flow area of the regurgitant jet is not recommended to quantify the severity of TR. The colour flow imaging should only be used for diagnosing TR. A more quantitative approach is required when more than a small central TR jet is observed.

Vena contracta width

The vena contracta of the TR is typically imaged in the apical four-chamber view using the same settings as for MR (Figure 29). Averaging measurements over at least two to three beats is recommended. A vena contracta $\geq 7 \text{ mm}$ is in favour of severe TR although a diameter $<6 \text{ mm}$ is a strong argument in favour of

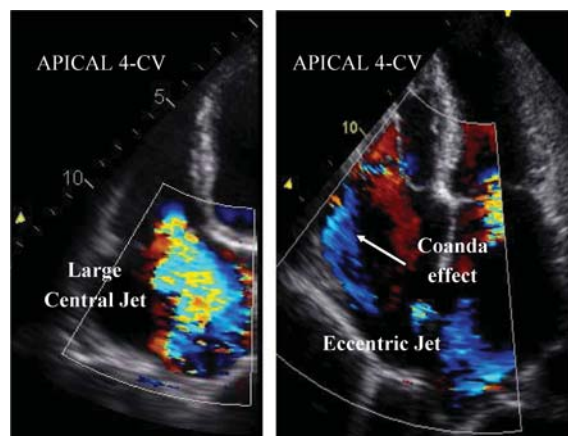


Figure 28 Visual assessment of tricuspid regurgitant jet using colour-flow imaging. (A) Large central jet; (B) eccentric jet with a clear Coanda effect. CV, four-chamber view.

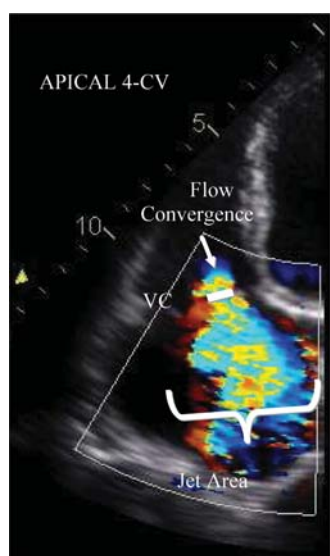


Figure 29 Semi-quantitative assessment of tricuspid regurgitation severity using the vena contracta width (VC). The three components of the regurgitant jet (flow convergence zone, vena contracta, jet turbulence) are obtained. CV, chamber view.

mild or moderate TR.⁵⁴ Intermediate values are not accurate at distinguishing moderate from mild TR. As for MR, the regurgitant orifice geometry is complex and not necessarily circular. A poor correlation has been suggested between the 2D vena contracta width and the 3D assessment of the EROA. This could underline the poor accuracy of the 2D vena contracta width in eccentric jets. With 3D echo, an EROA $> 75 \text{ mm}^2$ seems to indicate severe TR.⁵⁵ However, these data need to be confirmed in further studies.

Key point

When feasible, the measurement of the vena contracta width is recommended to quantify TR. A vena contracta width

$\geq 7 \text{ mm}$ defines severe TR. Lower values are difficult to interpret. In case of multiple jets, the respective values of the vena contracta width are not additive. The assessment of the vena contracta by 3D echo is still reserved to research purposes.

The flow convergence method

Although providing quantitative assessment, clinical practice reveals that the flow convergence method is rarely applied in TR. This approach has been validated in small studies.^{56–58} The apical four-chamber view and the parasternal long and short axis views are classically recommended for optimal visualization of the PISA. The area of interest is optimized by lowering imaging depth and the Nyquist limit to $\sim 15\text{--}40 \text{ cm/s}$. The radius of the PISA is measured at mid-systole using the first aliasing (Figure 30). Qualitatively, a TR PISA radius $> 9 \text{ mm}$ at a Nyquist limit of 28 cm/s alerts to the presence of significant TR whereas a radius $< 5 \text{ mm}$ suggests mild TR.⁵⁷ An EROA $\geq 40 \text{ mm}^2$ or a R Vol of $\geq 45 \text{ mL}$ indicates severe TR. As mentioned in the first part of the recommendations on the assessment of valvular regurgitation, the PISA method faces several advantages and limitations.¹ It could underestimate the severity of TR by 30%. This method is also less accurate in eccentric jets. To note, the number of studies having evaluated the value of the flow convergence method in TR are still limited.

Key point

When feasible, the PISA method is reasonable to quantify the TR severity. An EROA $\geq 40 \text{ mm}^2$ or a R Vol $\geq 45 \text{ mL}$ indicates severe TR.

Pulsed Doppler

Doppler volumetric method

Quantitative PW Doppler method is rarely used to quantify the TR severity. As for MR, this approach is time consuming and is associated with several drawbacks (see above).

Anterograde velocity of tricuspid inflow

Similar to MR, the severity of TR will affect the early tricuspid diastolic filling (*E* velocity). In the absence of tricuspid stenosis, the peak *E* velocity increases in proportion to the degree of TR. Tricuspid inflow Doppler tracings are obtained at the tricuspid leaflet tips. A peak *E* velocity $\geq 1 \text{ m/s}$ suggests severe TR (Figure 31).

Hepatic vein flow

Pulsed Doppler evaluation of hepatic venous flow pattern is another aid for grading TR. In normal individuals, the pattern of flow velocity consists of antegrade systolic, transient flow reversal as the TV annulus recoils at the end of systole, antegrade diastolic and a retrograde A wave caused by atrial contraction. Such hepatic flow patterns are affected by respiration. With increasing severity of TR, there is a decrease in hepatic vein systolic velocity. In severe TR, systolic flow reversal occurs (Figure 32). The sensitivity of flow reversal for severe TR is 80%.⁵³ Thus, the absence of systolic flow reversal does not rule out severe TR. Blunted systolic hepatic vein flow can be observed in case of abnormal right atrial and RV compliance, atrial fibrillation and elevated right atrial pressure from any cause.⁵⁹ Blunting of hepatic flow may thus lack of specificity.

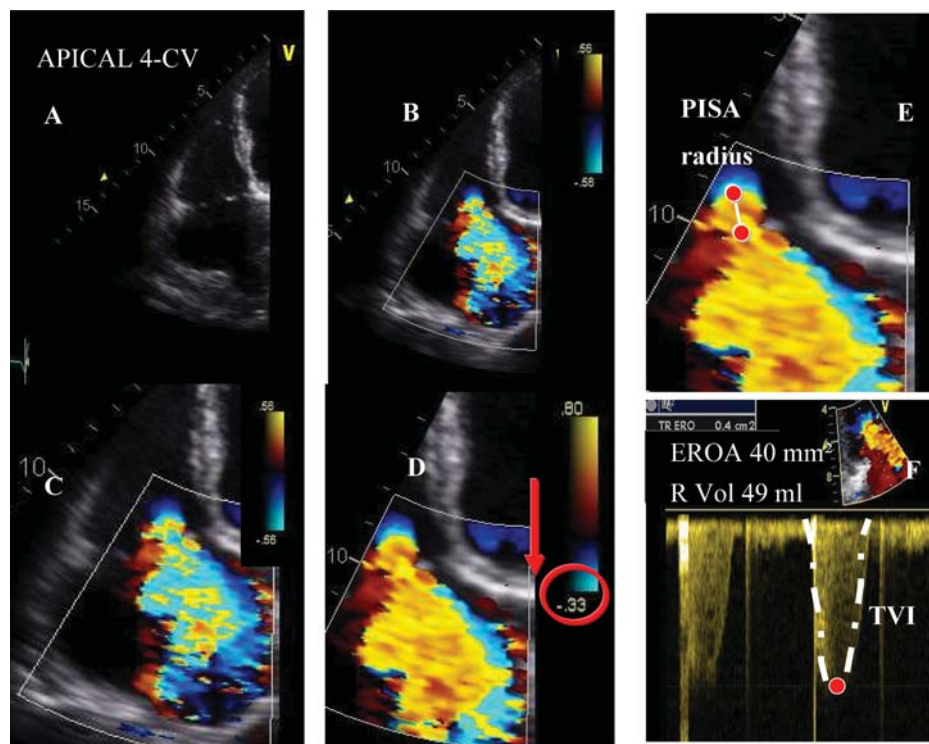


Figure 30 Quantitative assessment of TR severity using the proximal isovelocity surface area (PISA) method. Stepwise analysis of mitral regurgitation: (A) Apical four-chamber view (CV); (B) colour-flow display; (C) zoom of the selected zone; (D) downward shift of zero baseline to obtain an hemispheric PISA; (E) measure of the PISA radius using the first aliasing; (F) continuous wave Doppler of tricuspid regurgitation jet allowing calculation the effective regurgitant orifice area (EROA) and regurgitant volume (R Vol). TVI, time-velocity integral.

Retrograde systolic flow can also be seen with colour flow Doppler. It can be associated with phasic spontaneous appearance of some contrast in the hepatic vein.

Key point

The systolic hepatic flow reversal is specific for severe TR. It represents the strongest additional parameter for evaluating the severity of TR.

Continuous wave Doppler of tricuspid regurgitation jet

Signal intensity and shape

As for MR, the CW envelope of the TR jet can be a guide to TR severity. A dense TR signal with a full envelope indicates more severe TR than a faint signal. The CW Doppler envelope may be truncated (notch) with a triangular contour and an early peak velocity (blunt). This indicates elevated right atrial pressure or a prominent regurgitant pressure wave in the RA due to severe TR. Marked respiratory variation (decreased TR velocity with inspiration) suggests an elevated RA pressure (Kussmaul's sign on physical examination).

Pulmonary artery pressure

The TR jet can be used to determine RV or pulmonary artery systolic pressure. This is done by calculating the RV to RA pressure gradient using the modified Bernoulli equation and then adding an assumed RA pressure. Details on how to assess pulmonary pressure will be provided in other recommendations. To note,

the velocity of the TR jet by itself does not provide useful information about the severity of TR. For instance, massive TR is often associated with a low jet velocity (<2 m/s) as there is near equalization of RV and RA pressures.⁶⁰ In some case, a high-velocity jet that represents only mild TR may be present when severe pulmonary hypertension is present.

Consequences of tricuspid regurgitation

Signs of severe TR include RA and RV dilatation, a dilated and pulsatile inferior vena cava and hepatic vein, a dilated coronary sinus and systolic bowing of the interatrial septum toward the LA. Evidence of right heart dilatation is not specific for TR but can be noted in other conditions (pulmonary valve regurgitation, left-to-right atrial shunt, anomalous venous return). However, its absence suggests milder degree of TR. Imaging the vena cava and its respiratory variation also provides an evaluation of RA pressure. Although not specific, a rapid anterior motion of the interventricular septum at the onset of systole (isovolumic contraction; paradoxical ventricular septal motion) represents a qualitative sign of RV volume overload due to severe TR.

Right ventricle size and function

Similar to LV, the RV dimensions and ejection fraction reflect the right heart's ability to adapt to increased volume load. In case of TR, significant changes in RV shape can occur. An end-systolic RV eccentricity index greater than two—obtained by dividing the

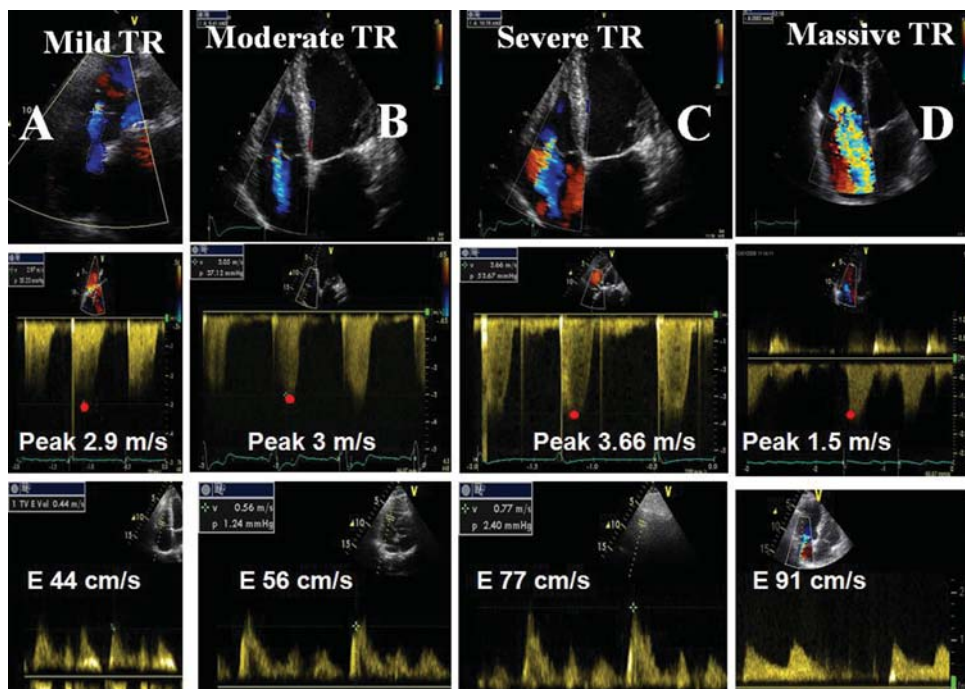


Figure 31 Four examples of various degrees of tricuspid regurgitation (TR), mild (A), moderate (B), severe (C), and massive (D) are provided. The regurgitant jet area (RJA) as well as the tricuspid E wave velocity increase with the severity of TR. In severe TR, the continuous wave Doppler signal of the regurgitant jet is truncated, triangular and intense. The peak velocity of TR (continuous wave Doppler) allows the estimation of pulmonary pressure except in case of massive TR, since the Bernoulli equation is not applicable.

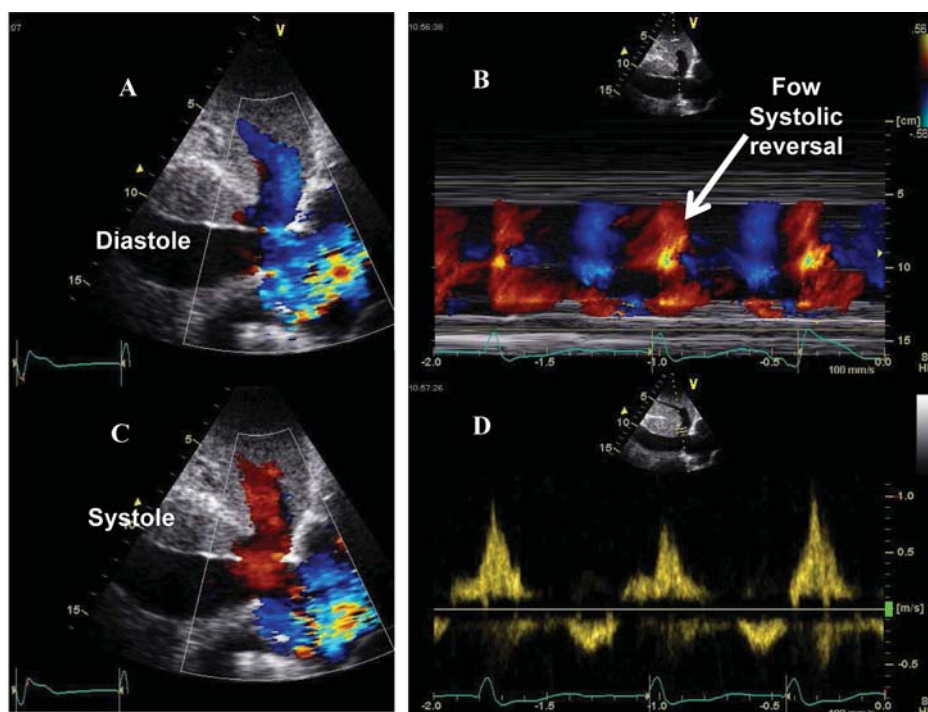


Figure 32 Subcostal echocardiogram recorded in a patient with severe tricuspid regurgitation. (A–C) The colour Doppler confirms retrograde flow into the vena cava and hepatic vein in systole consistent with TR (red). (D) A spectral Doppler recording from a hepatic vein, also confirming the systolic retrograde flow.

Table 5 Grading the severity of TR

Parameters	Mild	Moderate	Severe
Qualitative			
Tricuspid valve morphology	Normal/abnormal	Normal/abnormal	Abnormal/flail/large coaptation defect
Colour flow TR jet ^a	Small, central	Intermediate	Very large central jet or eccentric wall impinging jet
CW signal of TR jet	Faint/Parabolic	Dense/Parabolic	Dense/Triangular with early peaking (peak <2 m/s in massive TR)
Semi-quantitative			
VC width (mm) ^a	Not defined	<7	≥7
PISA radius (mm) ^b	≤5	6–9	>9
Hepatic vein flow ^c	Systolic dominance	Systolic blunting	Systolic flow reversal
Tricuspid inflow	Normal	Normal	E wave dominant (≥1 cm/s) ^d
Quantitative			
EROA (mm ²)	Not defined	Not defined	≥40
R Vol (mL)	Not defined	Not defined	≥45
+ RA/RV/IVC dimension ^e			

CW, continuous-wave; EROA, effective regurgitant orifice area; RA, right atrium; RV, right ventricle; R Vol, regurgitant volume; TR, tricuspid regurgitation; VC, vena contracta.

^aAt a Nyquist limit of 50–60 cm/s.

^bBaseline Nyquist limit shift of 28 cm/s.

^cUnless other reasons of systolic blunting (atrial fibrillation, elevated RA pressure).

^dIn the absence of other causes of elevated RA pressure.

^eUnless for other reasons, the RA and RV size and IVC are usually normal in patients with mild TR. An end-systolic RV eccentricity index >2 is in favour of severe TR. In acute severe TR, the RV size is often normal. In chronic severe TR, the RV is classically dilated. Accepted cut-off values for non significant right-sided chambers enlargement (measurements obtained from the apical four-chamber view): Mid RV dimension ≤33 mm, RV end-diastolic area ≤28 cm², RV end-systolic area ≤16 cm², RV fractional area change >32%, maximal RA volume ≤33 mL/m².

An IVC diameter <1.5 cm is considered normal.

longest right lateral distance by the distance connecting the ventricular septum and the RV free wall—is in favour of severe TR (sensitivity of 79%).⁵⁰ Conversely, it has been reported a poor correlation between the RV area, the fractional area change and the degree of TR. RV dysfunction may be seen in both left-sided and right-sided valvular heart disease. In unoperated patients with mitral valve disease, subnormal RV ejection fraction at rest is associated with decreased exercise tolerance and mortality. In operated patients, a RV ejection fraction <20% predicted post-operative death.⁶¹ Progressive RV dysfunction may also result from chronic TR. In a recent study, it has been shown that flail tricuspid valve is associated with decreased survival and increasing risk of heart failure.⁶² This indicates that sustained severe TR for a long time could lead to significant RV muscle dysfunction. As for the LV, the RV ejection fraction is a crude estimate of RV function. It is dependent on loading conditions, ventricular interaction as well as myocardial structure. New parameters are currently available for a better assessment of RV function but they still need to be validated in both left and right-sided valve diseases. A tricuspid annular plane systolic excursion (TAPSE) <8.5 mm (M-mode line placed at the level of lateral tricuspid annulus on apical four-chamber view) correlates with a RV ejection fraction of <25%. A TAPSE <15 mm is considered as significantly reduced. A systolic tissue Doppler velocity measured at the lateral tricuspid annulus <11 cm/s correlates with a RV ejection fraction of <45%.⁶³ Both the TAPSE and the systolic velocity are less accurate in patients with severe TR.⁶⁴ Little is known about the value of myocardial acceleration during isovolumic contraction and RV strain in valvular regurgitation.

Key point

When TR is more than mild TR, the evaluation of RV dimensions and function, RA volume, inferior vena cava diameter and the pulmonary arterial systolic pressure is mandatory.¹ The assessment of myocardial function by using the TAPSE or the systolic myocardial velocities is reasonable to identify subtle RV dysfunction.

Role of exercise echocardiography

As for MR, the goal of exercise echocardiography is to examine the RV functional reserve and to evaluate the changes in pulmonary artery systolic pressure. No data are currently available on patients with isolated TR.

Integrating indices of severity

Echocardiographic assessment of TR includes integration of data from 2D/3D imaging of the valve, right heart chambers, septal motion and inferior vena cava as well as Doppler measures of regurgitant severity (Table 5). Colour flow Doppler should be examined in multiple windows. The consensus of the expert is to advocate grading the severity of TR by using the vena contracta width and the PISA method, except in the presence of mild or less TR. However, as extensive data on the usefulness of these approaches are still lacking, the experts also recommend corroborating the results of these methods with the other available parameters. Advantages and limitations of the various echo Doppler parameters used in assessing TR severity are detailed in Table 6.

Table 6 Echocardiographic parameters used to quantify tricuspid regurgitation severity: recordings, advantages, and limitations

Parameters	Recordings	Usefulness/advantages	Limitations
Tricuspid valve morphology	<ul style="list-style-type: none"> • Visual assessment • Multiple views 	<ul style="list-style-type: none"> • Flail valve is specific for significant TR 	<ul style="list-style-type: none"> • Other abnormalities are non-specific of significant TR
Tricuspid annulus diameter	<ul style="list-style-type: none"> • Apical four-chamber view • Lateral inner edge to septal inner edge 	<ul style="list-style-type: none"> • Dilatation sensitive for severe TR 	<ul style="list-style-type: none"> • Dilatation seen in other conditions • Need to be confirmed in further studies
Colour flow TR jet	<ul style="list-style-type: none"> • Optimize colour gain/scale • Evaluate in two views • Need blood pressure evaluation 	<ul style="list-style-type: none"> • Ease of use • Evaluates the spatial orientation of TR jet • Good screening test for mild vs. severe TR 	<ul style="list-style-type: none"> • Can be inaccurate for estimation of TR severity • Influenced by technical and haemodynamic factors • Underestimates eccentric jet adhering the RA wall (Coanda effect)
VC width	<ul style="list-style-type: none"> • Apical four-chamber view • Optimize colour gain/scale • Identify the three components of the regurgitant jet (VC, PISA, Jet into RA) • Reduce the colour sector size and imaging depth to maximize frame rate • Expand the selected zone (Zoom) • Use the cine-loop to find the best frame for measurement • Measure the smallest VC (immediately distal to the regurgitant orifice, perpendicular to the direction of the jet) 	<ul style="list-style-type: none"> • Relatively quick and easy • Relatively independent of haemodynamic and instrumentation factors • Not affected by other valve leak • Good for extremes TR: mild vs. severe • Can be used in eccentric jet 	<ul style="list-style-type: none"> • Not valid for multiple jets • Small values; small measurement errors leads to large % error • Intermediate values need confirmation • Affected by systolic changes in regurgitant flow
PISA method	<ul style="list-style-type: none"> • Apical four-chamber • Optimize colour flow imaging of TR • Zoom the image of the regurgitant tricuspid valve • Decrease the Nyquist limit (colour flow zero baseline) • With the cine mode select the best PISA • Display the colour off and on to visualize the TR orifice • Measure the PISA radius at mid-systole using the first aliasing and along the direction of the ultrasound beam • Measure TR peak velocity and TVI (CW) • Calculate flow rate, EROA, R Vol 	<ul style="list-style-type: none"> • Can be used in eccentric jet • Not affected by the aetiology of TR or other valve leak • Quantitative: estimate lesion severity (EROA) and volume overload (R Vol) • Large flow convergence at 28 cm/s alerts to significant TR 	<ul style="list-style-type: none"> • PISA shape affected <ul style="list-style-type: none"> – by the aliasing velocity – in case of non-circular orifice – by systolic changes in regurgitant flow – by adjacent structures (flow constraint) • Errors in PISA radius measurement are squared • Inter-observer variability • Validated in only few studies
CW TR jet profile	<ul style="list-style-type: none"> • Apical four-chamber 	<ul style="list-style-type: none"> • Simple, easily available 	<ul style="list-style-type: none"> • Qualitative, Complementary finding • Complete signal difficult to obtain in eccentric jet
Hepatic vein flow	<ul style="list-style-type: none"> • Subcostal view • Sample volume of PW places into the hepatic vein 	<ul style="list-style-type: none"> • Simple • Systolic flow reversal is specific for severe TR 	<ul style="list-style-type: none"> • Affected by RA pressure, atrial fibrillation
Peak E velocity	<ul style="list-style-type: none"> • Apical four-chamber • Sample volume of PW places at tricuspid leaflet tips 	<ul style="list-style-type: none"> • Simple, easily available • Usually increased in severe TR 	<ul style="list-style-type: none"> • Affected by RA pressure, atrial fibrillation, RV relaxation • Complementary finding

Continued

Table 6 Continued

Parameters	Recordings	Usefulness/advantages	Limitations
Atrial and RV size	<ul style="list-style-type: none"> Use preferably the RV dimension from the apical four-chamber view 	<ul style="list-style-type: none"> Dilatation sensitive for chronic significant TR Normal size almost excludes significant chronic TR 	<ul style="list-style-type: none"> Dilatation observed in other conditions (non specific) May be normal in acute severe TR

CW, continuous-wave; RA, right atrium; EROA, effective regurgitant orifice area; RV, right ventricle; TR, tricuspid regurgitation; PW, pulse wave; R Vol, regurgitant volume; VC, vena contracta.

Recommended follow-up

As for other valvular regurgitation, the follow-up of patients with TR depends on the aetiology and severity of TR, the RV size and function and the associated diseases. Usually, the follow-up will be dictated by the severity of left-sided valve disease. Although data are limited, careful follow-up should be organized in patients with moderate to severe TR.

Conflict of interest: none declared.

References

- Lancellotti P, Tribouilloy C, Hagendorff A, Moura L, Popescu BA, Agricola E *et al.* on behalf of the European Association of Echocardiography. European Association of Echocardiography recommendations for the assessment of valvular regurgitation. Part 1: aortic and pulmonary regurgitation (native valve disease). *Eur J Echocardiogr* 2010;**11**:223–44.
- Vahanian A, Baumgartner H, Bax J, Butchart E, Dion R, Filippatos G *et al.* Guidelines on the management of valvular heart disease: the task force on the management of valvular heart disease of the European society of cardiology. *Eur Heart J* 2007;**28**:230–68.
- O’Gara P, Sugeng L, Lang R, Sarano M, Hung J, Raman S *et al.* The role of imaging in chronic degenerative mitral regurgitation. *JACC Cardiovasc Imaging* 2008;**1**:221–37.
- Monin JL, Dehant P, Roiron C, Monchi M, Tabet JY, Clerc P *et al.* Functional assessment of mitral regurgitation by transthoracic echocardiography using standardized imaging planes diagnostic accuracy and outcome implications. *J Am Coll Cardiol* 2005;**46**:302–9.
- Macnab A, Jenkins NP, Bridgewater BJ, Hooper TL, Greenhalgh DL, Patrick MR *et al.* Three-dimensional echocardiography is superior to multiplane transoesophageal echo in the assessment of regurgitant mitral valve morphology. *Eur J Echocardiogr* 2004;**5**:212–22.
- Daimon M, Saracino G, Gillinov AM, Koyama Y, Fukuda S, Kwan J *et al.* Local dysfunction and asymmetrical deformation of mitral annular geometry in ischemic mitral regurgitation: a novel computerized 3D echocardiographic analysis. *Echocardiography* 2008;**25**:414–23.
- Caldarera I, Van Herwerden LA, Taams MA, Bos E, Roelandt JR. Multiplane transoesophageal echocardiography and morphology of regurgitant mitral valves in surgical repair. *Eur Heart J* 1995;**16**:999–1006.
- Lancellotti P, Lebrun F, Piérard LA. Determinants of exercise-induced changes in mitral regurgitation in patients with coronary artery disease and left ventricular dysfunction. *J Am Coll Cardiol* 2003;**42**:1921–8.
- Marwick TH, Lancellotti P, Piérard L. Ischaemic mitral regurgitation: mechanisms and diagnosis. *Heart* 2009;**95**:1711–8.
- Agricola E, Oppizzi M, Pisani M, Meris A, Maisano F, Margonato A. Ischemic mitral regurgitation: mechanisms and echocardiographic classification. *Eur J Echocardiogr* 2008;**9**:207–21.
- Lancellotti P, Marwick T, Piérard LA. How to manage ischaemic mitral regurgitation. *Heart* 2008;**94**:1497–502.
- Omran AS, Woo A, David TE, Feindel CM, Rakowski H, Siu SC. Intraoperative transoesophageal echocardiography accurately predicts mitral valve anatomy and suitability for repair. *J Am Soc Echocardiogr* 2002;**15**:950–7.
- Kongsarepong V, Shiota M, Gillinov AM, Song JM, Fukuda S, McCarthy PM *et al.* Echocardiographic predictors of successful versus unsuccessful mitral valve repair in ischemic mitral regurgitation. *Am J Cardiol* 2006;**98**:504–8.
- Chaliki HP, Nishimura RA, Enriquez-Sarano M, Reeder GS. A simplified, practical approach to assessment of severity of mitral regurgitation by Doppler color flow imaging with proximal convergence: validation with concomitant cardiac catheterization. *Mayo Clin Proc* 1998;**73**:929–35.
- McCully RB, Enriquez-Sarano M, Tajik AJ, Seward JB. Overestimation of severity of ischemic/functional mitral regurgitation by color Doppler jet area. *Am J Cardiol* 1994;**74**:790–3.
- Tribouilloy C, Shen WF, Quéré JP, Rey JL, Choquet D, Dufossé H *et al.* Assessment of severity of mitral regurgitation by measuring regurgitant jet width at its origin with transesophageal Doppler color flow imaging. *Circulation* 1992;**85**:1248–53.
- Heinle SK, Hall SA, Brickner ME, Willett DL, Grayburn PA. Comparison of vena contracta width by multiplane transesophageal echocardiography with quantitative Doppler assessment of mitral regurgitation. *Am J Cardiol* 1998;**81**:175–9.
- Hall SA, Brickner ME, Willett DL, Irani WN, Afridi I, Grayburn PA. Assessment of mitral regurgitation severity by Doppler color flow mapping of the vena contracta. *Circulation* 1997;**95**:636–42.
- Matsumura Y, Fukuda S, Tran H, Greenberg NL, Agler DA, Wada N *et al.* Geometry of the proximal isovelocity surface area in mitral regurgitation by 3-dimensional color Doppler echocardiography: difference between functional mitral regurgitation and prolapse regurgitation. *Am Heart J* 2008;**155**:231–8.
- Song JM, Kim MJ, Kim YJ, Kang SH, Kim JJ, Kang DH *et al.* Three-dimensional characteristics of functional mitral regurgitation in patients with severe left ventricular dysfunction: a real-time three-dimensional colour Doppler echocardiography study. *Heart* 2008;**94**:590–6.
- Yosefy C, Hung J, Chua S, Vaturi M, Ton-Nu TT, Handschumacher MD *et al.* Direct measurement of vena contracta area by real-time 3-dimensional echocardiography for assessing severity of mitral regurgitation. *Am J Cardiol* 2009;**104**:978–83.
- Kahlert P, Plicht B, Schenk IM, Janosi RA, Erbel R, Buck T. Direct assessment of size and shape of noncircular vena contracta area in functional versus organic mitral regurgitation using real-time three-dimensional echocardiography. *J Am Soc Echocardiogr* 2008;**21**:912–21.
- Khanna D, Vengala S, Miller AP, Nanda NC, Lloyd SG, Ahmed S *et al.* Quantification of mitral regurgitation by live three-dimensional transthoracic echocardiographic measurements of vena contracta area. *Echocardiography* 2004;**21**:737–43.
- Enriquez-Sarano M, Avierinos JF, Messika-Zeitoun D, Detaint D, Capps M, Nkomo V *et al.* Quantitative determinants of the outcome of asymptomatic mitral regurgitation. *N Engl J Med* 2005;**352**:875–83.
- Lancellotti P, Troisfontaines P, Toussaint AC, Piérard LA. Prognostic importance of exercise-induced changes in mitral regurgitation in patients with chronic ischemic left ventricular dysfunction. *Circulation* 2003;**108**:1713–7.
- Enriquez-Sarano M, Miller FA Jr, Hayes SN, Bailey KR, Tajik AJ, Seward JB. Effective mitral regurgitant orifice area: clinical use and pitfalls of the proximal isovelocity surface area method. *J Am Coll Cardiol* 1995;**25**:703–9.
- Schwammenthal E, Popescu AC, Popescu BA, Freimark D, Hod H, Eldar M *et al.* Mechanism of mitral regurgitation in inferior wall acute myocardial infarction. *Am J Cardiol* 2002;**90**:306–9.
- Iwakura K, Ito H, Kawano S, Okamura A, Kurotobi T, Date M *et al.* Comparison of orifice area by transthoracic three-dimensional Doppler echocardiography versus proximal isovelocity surface area (PISA) method for assessment of mitral regurgitation. *Am J Cardiol* 2006;**97**:1630–7.
- Dujardin KS, Enriquez-Sarano M, Bailey KR, Nishimura RA, Seward JB, Tajik AJ. Grading of mitral regurgitation by quantitative Doppler echocardiography: calibration by left ventricular angiography in routine clinical practice. *Circulation* 1997;**96**:3409–15.

30. Tribouilloy C, Shen WF, Rey JL, Adam MC, Lesbre JP. Mitral to aortic velocity-time integral ratio. A non-geometric pulsed-Doppler regurgitant index in isolated pure mitral regurgitation. *Eur Heart J* 1994;**15**:1335–9.
31. Enriquez-Sarano M, Dujardin KS, Tribouilloy CM, Seward JB, Yoganathan AP, Bailey KR et al. Determinants of pulmonary venous flow reversal in mitral regurgitation and its usefulness in determining the severity of regurgitation. *Am J Cardiol* 1999;**83**:535–41.
32. Bonow RO, Carabello BA, Chatterjee K, de Leon AC Jr, Faxon DP, Freed MD et al. 2008 Focused update incorporated into the ACC/AHA 2006 guidelines for the management of patients with valvular heart disease. *Circulation* 2008;**118**:e523–661.
33. Tribouilloy C, Grigioni F, Avierinos JF, Barbieri A, Rusinaru D, Szymanski C et al. MIDA Investigators. Survival implication of left ventricular end-systolic diameter in mitral regurgitation due to flail leaflets: a long-term follow-up multicenter study. *J Am Coll Cardiol* 2009;**54**:1961–8.
34. Agricola E, Galderisi M, Oppizzi M, Schinkel AF, Maisano F, De Bonis M et al. Pulsed tissue Doppler imaging detects early myocardial dysfunction in asymptomatic patients with severe mitral regurgitation. *Heart* 2004;**90**:406–10.
35. Marciniak A, Claus P, Sutherland GR, Marciniak M, Karu T, Baltabaeva A et al. Changes in systolic left ventricular function in isolated mitral regurgitation. A strain rate imaging study. *Eur Heart J* 2007;**28**:2627–36.
36. Lee R, Marwick TH. Assessment of subclinical left ventricular dysfunction in asymptomatic mitral regurgitation. *Eur J Echocardiogr* 2007;**8**:175–84.
37. Lancellotti P, Cosyns B, Zacharakis D, Attena E, Van Camp G, Gach O et al. Importance of left ventricular longitudinal function and functional reserve in patients with degenerative mitral regurgitation: assessment by 2-D speckle tracking. *J Am Soc Echocardiogr* 2008;**21**:1331–6.
38. Messika-Zeitoun D, Bellamy M, Avierinos JF, Breen J, Eusemann C, Rossi A et al. Left atrial remodelling in mitral regurgitation—methodologic approach, physiological determinants, and outcome implications: a prospective quantitative Doppler-echocardiographic and electron beam-computed tomographic study. *Eur Heart J* 2007;**28**:1773–81.
39. Antonini-Canterin F, Beladan CC, Popescu BA, Ghingina C, Popescu AC, Piazza R et al. Left atrial remodelling early after mitral valve repair for degenerative mitral regurgitation. *Heart* 2008;**94**:759–64.
40. Sicari R, Nihoyannopoulos P, Evangelista A, Kasprzak J, Lancellotti P, Poldermans D et al. European Association of Echocardiography. Stress echocardiography expert consensus statement: European Association of Echocardiography (EAE) (a registered branch of the ESC). *Eur J Echocardiogr* 2008;**9**:415–37.
41. Lebrun F, Lancellotti P, Piérard LA. Quantitation of functional mitral regurgitation during bicycle exercise in patients with heart failure. *J Am Coll Cardiol* 2001;**38**:1685–92.
42. Piérard LA, Lancellotti P. The role of ischemic mitral regurgitation in the pathogenesis of acute pulmonary edema. *N Engl J Med* 2004;**35**:1627–34.
43. Lancellotti P, Gérard P, Piérard LA. Long-term outcome of patients with heart failure and dynamic functional mitral regurgitation. *Eur Heart J* 2005;**26**:1528–32.
44. Enriquez-Sarano M, Basmadjian AJ, Rossi A, Bailey KR, Seward JB, Tajik AJ. Progression of mitral regurgitation: a prospective Doppler echocardiographic study. *J Am Coll Cardiol* 1999;**34**:1137–44.
45. Rogers JH, Bolling SF. The tricuspid valve: current perspective and evolving management of tricuspid regurgitation. *Circulation* 2009;**119**:2718–25.
46. Badano LP, Agricola E, Perez de Isla L, Gianfagna P, Zamorano JL. Evaluation of the tricuspid valve morphology and function by transthoracic real-time three-dimensional echocardiography. *Eur J Echocardiogr* 2009;**10**:477–84.
47. Schnabel R, Khaw AV, von Bardeleben RS, Strasser C, Kramm T, Meyer J et al. Assessment of the tricuspid valve morphology by transthoracic real-time-3D-echocardiography. *Echocardiography* 2005;**22**:15–23.
48. Kwan J, Kim GC, Jeon MJ, Kim DH, Shiota T, Thomas JD et al. 3D geometry of a normal tricuspid annulus during systole: a comparison study with the mitral annulus using real-time 3D echocardiography. *Eur J Echocardiogr* 2007;**8**:375–83.
49. Shiran A, Sagie A. Tricuspid regurgitation in mitral valve disease: incidence, prognostic implications, mechanism, and management. *J Am Coll Cardiol* 2009;**53**:401–8.
50. Kim HK, Kim YJ, Park JS, Kim KH, Kim KB, Ahn H et al. Determinants of the severity of functional tricuspid regurgitation. *Am J Cardiol* 2006;**98**:236–42.
51. Matsunaga A, Duran CM. Progression of tricuspid regurgitation after repaired functional ischemic mitral regurgitation. *Circulation* 2005;**112**:1453–7.
52. Fukuda S, Gillinov AM, McCarthy PM, Stewart WJ, Song JM, Kihara T et al. Determinants of recurrent or residual functional tricuspid regurgitation after tricuspid annuloplasty. *Circulation* 2006;**114**:1582–7.
53. Gonzalez-Vilchez F, Zarauza J, Vazquez de Prada JA, Martín Durán R, Ruano J, Delgado C et al. Assessment of tricuspid regurgitation by Doppler color flow imaging: angiographic correlation. *Int J Cardiol* 1994;**44**:275–83.
54. Tribouilloy CM, Enriquez-Sarano M, Bailey KR, Tajik AJ, Seward JB. Quantification of tricuspid regurgitation by measuring the width of the vena contracta with Doppler color flow imaging: a clinical study. *J Am Coll Cardiol* 2000;**36**:472–8.
55. Velayudhan DE, Brown TM, Nanda NC, Patel V, Miller AP, Mehmood F et al. Quantification of tricuspid regurgitation by live three-dimensional transthoracic echocardiographic measurements of vena contracta area. *Echocardiography* 2006;**23**:793–800.
56. Rivera JM, Vandervoort P, Mele D, Weyman A, Thomas JD. Value of proximal regurgitant jet size in tricuspid regurgitation. *Am Heart J* 1996;**131**:742–7.
57. Tribouilloy CM, Enriquez-Sarano M, Capps MA, Bailey KR, Tajik AJ. Contrasting effect of similar effective regurgitant orifice area in mitral and tricuspid regurgitation: a quantitative Doppler echocardiographic study. *J Am Soc Echocardiogr* 2002;**15**:958–65.
58. Grossmann G, Stein M, Kochs M, Höher M, Koenig W, Hombach V et al. Comparison of the proximal flow convergence method and the jet area method for the assessment of the severity of tricuspid regurgitation. *Eur Heart J* 1998;**19**:652–9.
59. Nagueh SF, Kopelen HA, Zoghbi WA. Relation of mean right atrial pressure to echocardiographic and Doppler parameters of right atrial and right ventricular function. *Circulation* 1996;**93**:1160–9.
60. Minagoe S, Rahimtoola SH, Chandraratna PA. Significance of laminar systolic regurgitant flow in patients with tricuspid regurgitation: a combined pulsed-wave, continuous-wave Doppler and two-dimensional echocardiographic study. *Am Heart J* 1990;**119**:627–35.
61. Dini FL, Conti U, Fontanive P, Andreini D, Banti S, Braccini L et al. Right ventricular dysfunction is a major predictor of outcome in patients with moderate to severe mitral regurgitation and left ventricular dysfunction. *Am Heart J* 2007;**154**:172–9.
62. Messika-Zeitoun D, Thomson H, Bellamy M, Scott C, Tribouilloy C, Dearani J et al. Medical and surgical outcome of tricuspid regurgitation caused by flail leaflets. *J Thorac Cardiovasc Surg* 2004;**128**:296–302.
63. Haddad F, Doyle R, Murphy DJ, Hunt SA. Right ventricular function in cardiovascular disease, part II: pathophysiology, clinical importance, and management of right ventricular failure. *Circulation* 2008;**117**:1717–31.
64. Hsiao SH, Lin SK, Wang WC, Yang SH, Gin PL, Liu CP. Severe tricuspid regurgitation shows significant impact in the relationship among peak systolic tricuspid annular velocity, tricuspid annular plane systolic excursion, and right ventricular ejection fraction. *J Am Soc Echocardiogr* 2006;**19**:902–10.